2011

Economic analysis for transmission operation and planning

Qun Zhou
Iowa State University

Economic analysis for transmission operation and planning

by

Qun Zhou

A dissertation submitted to the graduate faculty

in partial fulfillment of the requirements for the degree of

DOCTOR OF PHILOSOPHY

Major: Electrical Engineering

Program of Study Committee:
Chen-Ching Liu, Co-major Professor
Leigh Tesfatsion, Co-major Professor
Venkataramana Ajjarapu
William Meeker
Lizhi Wang

Iowa State University

Ames, Iowa

2011

TABLE OF CONTENTS

LIST OF FIGURES iv

LIST OF TABLES v

ABSTRACT vii

CHAPTER 1. INTRODUCTION 1

1.1 Motivation and Objectives 1

1.2 Literature Review 5

1.2.1 Short-Term Transmission Congestion Forecasting 5

1.2.2 Transmission Investment for Integrating Renewable Energy 6

1.3 Contributions of this Dissertation 8

1.4 Thesis Organization 10

CHAPTER 2. SHORT-TERM TRANSMISSION CONGESTION FORECASTING 12

2.1 Introduction 12

2.2 Basic Forecasting Problem Formulation 14

2.3 Basic Forecasting Algorithm Description 16

2.3.1 System Patterns and System Pattern Regions 16

2.3.2 Convex Hull Estimation of Historical SPRs 19

2.3.3 Basic Point Inclusion Test 22

2.3.4 Linear-Affine Mapping Procedure 23

2.4 Extension to Probabilistic Forecasting 25

2.4.1 Practical Data Availability Issues 25

2.4.2 Probabilistic Point Inclusion Test 27

2.4.3 Probabilistic Forecasting Algorithm 30

2.5 Five-Bus System: Basic Forecasting 31

2.5.1 Historical System Patterns and the Corresponding Sensitivity Matrices 32

2.5.2 Predicting System Pattern, Congestion and System Variables 33

2.6 NYISO Case Study: Probabilistic Forecasting 36

2.6.1 Case Study Overview 36

2.6.2 Implementation of Probabilistic Forecasting 37

2.6.3 Congestion Pattern Forecasts 39

2.6.4 Mean Forecasts for LMPs 40

2.6.5 Interval Forecasts for Line Shadow Prices and LMPs 42
2.7 Extension to Cross-Scenario Forecasting 47

CHAPTER 3. TRANSMISSION INVESTMENT FOR INTEGRATING RENEWABLE ENERGY 49
3.1 Introduction 49
3.2 Nomenclature 50
3.3 Problem Formulation 51
3.3.1 Overview 51
3.3.2 Negotiation Process 52
3.3.3 Policy implications on RE subsidies 55
3.4 Negotiation: A Nash Bargaining Approach 55
3.4.1 Nash Bargaining 56
3.4.2 Bargaining on RE Interconnection: An Analytical Model 57
3.4.3 Bargaining on RE Interconnection: A Detailed Formulation 60
3.5 Implications on Renewable Subsidy Policy 63
3.5.1 Centralized Planning and Policy Implication 63
3.5.2 An Illustrative Example 64
3.5.3 Centralized Planning: A Detailed Formulation 68
3.6 Numerical Results 69
3.6.1 Garver's Six-Bus Test Case 69
3.6.2 The Negotiated Solution with Renewable Energy Contract Price *FP* 72
3.6.3 The Negotiated Solution with Market-Based Price *LMP* 73
3.6.4 Centralized Transmission Planning 74
3.6.5 RE Subsidy Sensitivity Analysis 75

CHAPTER 4. CONCLUSION 79
4.1 Summary of the Dissertation 79
4.2 Future Work 81

APPENDIX. PROOF 82

BIBLIOGRAPHY 86

LIST OF PUBLICATIONS 94

LIST OF FIGURES

Figure 1. Illustration of two system pattern regions (SPRs) in load space 19
Figure 2. Illustration of the QuickHull algorithm 21
Figure 3. Illustration of the basic point inclusion test for an SPR in a load plane 23
Figure 4. Convex hull estimates for SPRs can be biased 26
Figure 5. Two possible types of forecast error due to biased SPR estimates 27
Figure 6. 5-bus network 32
Figure 7. Predicted hourly power flow on line TL1 during day 363 35
Figure 8. Predicted LMP at bus 2 during day 363 35
Figure 9. Actual versus mean LMP forecasts for Zone Central on 01/31/2007 41
Figure 10. Actual versus mean LMP forecasts for Zone Central on 02/28/2007 41
Figure 11. Actual versus interval D-S line shadow price forecasts on 01/31/2007 43
Figure 12. Actual versus interval D-S line shadow price forecasts on 02/28/2007 44
Figure 13. Actual versus interval LMP forecasts for Zone Central on 01/31/2007 45
Figure 14. Actual versus interval LMP forecasts for Zone Central on 02/28/2007 46
Figure 15. Scenario-conditioned and cross-scenario forecasting 48
Figure 16. Negotiation between the RE-GenCo and the TransCo 54
Figure 17. Options for renewable generation and transmission investment 65
Figure 18. Garver's six-bus test system 70
Figure 19. Transmission plan variation under *SUB* with contract price *FP* 76
Figure 20. Transmission plan variation under *SUB* with market-based price *LMP* 77
Figure 21. Payment rate variation under *SUB* with contract price *FP* 77
Figure 22 Payment rate variation under *SUB* with market-based price *LMP* 78

LIST OF TABLES

Table 1. Flags used for system patterns 17
Table 2. The four most frequent historical system patterns for the 5-bus system 32
Table 3. Sensitivity matrix and ordinate vector for system pattern S4 (partially shown) 34
Table 4. LMP and line congestion predictions under S3 34
Table 5. Four most frequent historical congestion patterns for 01/31/2007 38
Table 6. Forecasted congestion patterns versus the actual pattern on 01/31/2007 40
Table 7. RMSE and MAPE values for the twelve test days 42
Table 8. Loss function values as a measure of interval forecasting performance 46
Table 9. Generator and load data 70
Table 10. Wind unit data 70
Table 11. Transmission data 71
Table 12. Scenarios of wind speed in four subperiods 72
Table 13. Maximum possible output of wind energy 72
Table 14. Negotiated transmission investment decision Y_N 73
Table 15. Negotiated results of payment rate and attained utilities 73
Table 16. Negotiated transmission plan Y_N^M and utility levels 74
Table 17. Centralized transmission investment decision Y_c 75
Table 18. Social surplus under different investment decisions 75

ACKNOWLEDGEMENTS

I would like to take this opportunity to express my deep and sincere gratitude to my major professors, Dr. Chen-Ching Liu and Dr. Leigh Tesfatsion. I have been fortunate to have Professor Liu as my advisor, who gave me the freedom to explore on my own and also the guidance that leads me towards the correct research direction. His patience and continuous support helped me accomplish this dissertation. I would also like to give my sincere thanks to Professor Tesfatsion. I am deeply grateful to her for the discussions that helped me sort out the technical details of my work. Besides being an inspiring advisor, she is also an excellent mentor in life, where she always gives me valuable advice, and her positive attitude has greatly influenced me in every aspect.

I am also grateful to my minor professor, Dr. William Meeker, for sharing his time to discuss research with me and also providing strong support in my career development.

I am also thankful to Dr. Lizhi Wang and Dr. Ajjarapu Venkataramana for their encouragement and valuable comments.

It is my pleasure to thank Dr. Ron Chu for the industry insights and enlightening discussion in this research.

I would also want to thank my dear husband, Wei Sun, for being there all the time. I am especially grateful to my parents, Chaoping Zhou and Suqin Wang, my sister and brother for their unconditional support and encouragement in my endeavors.

The author acknowledges the financial support of Electric Power Research Center (EPRC) at Iowa State University.

ABSTRACT

Restructuring of the electric power industry has caused dramatic changes in the use of transmission system. The increasing congestion conditions as well as the necessity of integrating renewable energy introduce new challenges and uncertainties to transmission operation and planning. Accurate short-term congestion forecasting facilitates market traders in bidding and trading activities. Cost sharing and recovery issue is a major impediment for long-term transmission investment to integrate renewable energy.

In this research, a new short-term forecasting algorithm is proposed for predicting congestion, LMPs, and other power system variables based on the concept of system patterns. The advantage of this algorithm relative to standard statistical forecasting methods is that structural aspects underlying power market operations are exploited to reduce the forecasting error. The advantage relative to previously proposed structural forecasting methods is that data requirements are substantially reduced. Forecasting results based on a NYISO case study demonstrate the feasibility and accuracy of the proposed algorithm.

Moreover, a negotiation methodology is developed to guide transmission investment for integrating renewable energy. Built on Nash Bargaining theory, the negotiation of investment plans and payment rate can proceed between renewable generation and transmission companies for cost sharing and recovery. The proposed approach is applied to Garver's six bus system. The numerical results demonstrate fairness and efficiency of the approach, and hence can be used as guidelines for renewable energy investors. The results also shed light on policy-making of renewable energy subsidies.

CHAPTER 1. INTRODUCTION

1.1 Motivation and Objectives

The integration of electricity markets and renewable energy into electric power systems continue to increase. Transmission operation and planning have become highly challenging in the new environment.

This research is aimed to tackle two challenging issues in transmission system operation and planning. Specifically, the first task is the development of a short-term congestion and price forecasting tool to facilitate bidding and trading strategy development for market participants. The proposed algorithm exploits both structural and statistical aspects of wholesale power markets, and outperforms state-of-the-art forecasting tools.

The second task is concerned with a new methodology to guide renewable energy generation and transmission companies on the negotiation of transmission investment cost sharing and recovery. The proposed approach based on Nash Bargaining theory gives a fair and efficient utility allocation in the negotiation process. The negotiation is further compared with a centralized planning model to provide guidance for policy makers on establishing appropriate renewable energy subsidies.

In many transmission regions, congestion in wholesale power markets is managed by Locational Marginal Prices (LMPs), the pricing of power in accordance with the location and timing of its power injection into or withdrawal from the transmission grid. Congestion and LMP forecasts are highly important for decision-making by market operators and market participants.

In short-term transmission operation, congestion occurs when the available economical electricity has to be delivered to load "out-of-merit-order" due to transmission limitations. Transmission congestion is detrimental to power system security. It also causes LMP discrepancies between the constrained and unconstrained areas, which could lead to a high congestion cost. Therefore, as a result of transmission congestion, high reliability risks and electricity price risks are faced by system operators and market participants, respectively.

Congestion forecasting is critical to market operators as well as market participants [1]. Congestion forecasting tools can be used for identification of potential congestive conditions, detection of the exercise of market power, and scenario-conditioned planning. Congestion forecasting also gives interpretable signals to electricity price behaviors, and can be used to induce more accurate and reliable price forecasting which assists market participants in making decisions for bidding and trading strategies. Therefore, accurate forecasts of congestion and LMP also give advantages to market traders in bidding and trading activities and long-term investment planning.[1]

In long-term system planning, major transmission projects are needed, in the United States and beyond, to integrate renewable resources, primarily wind generation, located mostly in remote areas. The delivery of renewable energy is important for meeting the Renewable Portfolio Standards (RPS). As of February 2009, nearly 300,000MW of wind projects were waiting to be connected to the grid [2]. One factor contributing to the backlog

[1] For example, during an internship at Genscape, Inc., the author observed first-hand that the customers for Genscape's LMP forecasting services were generation companies, load-serving entities, and utilities interested in developing daily market bidding strategies and improving their over-the-counter electricity trading.

is the difficulty in siting transmission lines due to local oppositions. For lines crossing multiple states, additional difficulties arise in the permitting process due to different state laws and regulations. However, the real issues are the uncertainties concerning who should bear the transmission costs and how the transmission investments should be recovered. In order to meet the RPS at the mandated date, these issues need to be resolved and transmission projects need to be completed.

Transmission can be separated into three categories; regulated, generation interconnection or merchant transmission. In general, the cost responsibility of the regulated transmission for reliability, economic and operational performance purposes is assigned to the loads benefiting from the investment via a regulated rate. The generation developers bear transmission cost for interconnecting its proposed generation and a transmission developer will be responsible for its merchant transmission project [3]. But the policy-driven transmission to meet RPS is a new category in which cost responsibility has not been clearly defined.

Currently, a RE developer has to pay the entire cost of the generation interconnection transmission to the interconnected Transmission Owner through a Regional Transmission Organization (RTO), such as PJM, ISO-New England, and New York ISO, prior to the in-service date of the generator. As a result, the RE developer bears the whole risk of both generation and transmission investments. This increases the cost to finance a RE project and discourage the investment. On the contrary, the authors propose a market-based approach, where the unavoidable risks and uncertainties due to renewable energy intermittency could be shared by RE developers and transmission companies. The expected generation revenue will be used to fund the RE and transmission projects.

In this dissertation, the interconnection of a RE project is accomplished by a Merchant Transmission (MT) project and is coordinated between a RE Generation Company (RE-GenCo) and a Transmission Company (TransCo). Furthermore, the recovery of their investments is a result of a negotiation between the two entities using the expected generation profit based on the market and generation performance. Hence, a RE-GenCo waiting to be connected to the power grid can actively seek out a TransCo who is interested in investing in new transmission lines if the compensation from the RE-GenCo is sufficiently attractive. Negotiation then can proceed considering the uncertainties associated with outputs renewable resources and electricity prices. An agreement is reached if satisfactory returns are achieved for both companies.

The prerequisite for a successful settlement from the negotiation between a RE-GenCo and a TransCo is the sufficient profit margins for both parties. However, it is possible that the expected generation revenue may not be adequate to cover the generation and transmission investments plus the profit margin. Under this situation, an incentive may be required to assure the accomplishment of these investments. However, if an incentive is needed, policy makers will have to deal with the questions, “What do the incentives look like and what would be their optimal values?” Schumacher *et al.* [4] report that incentive could be policy initiatives to promote transmission development. FERC also eases policies [5] for MT developers to hold auction to attract and pre-subscribe some capacity to “anchor customers.” Incentive can be monetary incentives such as Renewable Energy Certificates (RECs) that need to be purchased by LSEs to meet the RPS [6], or energy subsidies such as Investment Tax Credits (ITCs) and Production Tax Credits (PTCs). Using monetary incentives, RE-GenCos could gain an additional revenue stream that facilitates the negotiation process.

1.2 Literature Review

1.2.1 Short-Term Transmission Congestion Forecasting

Many studies have focused on electricity price forecasting. With only publicly available information in hand, most applicable price forecasting tools are restricted to statistical methods [1], [7]-[17]. For example, statistical methods are deployed to forecast the hourly Ontario energy price on a basis of publicly available electricity market information [7]. Nogales' research in [8] is a pioneering work in the application of time series models in electricity price forecasting. ARIMA [9] and GARCH [10] are also used to predict electricity price. Meanwhile, another branch in statistical forecasting has been developed based on intelligent system techniques, among which neural network approaches are widely used in load forecasting and extended to price forecasting as well. Shahidepour in [11] primarily focuses on the application of Artificial Neural Network (ANN) in load and price forecasting. Other neural network approaches [12]-[15] are also investigated in electricity price forecasting. Structural models considering wholesale power market fundamentals have also been attempted [19]-[20].

However, few studies have focused on congestion forecasting. Li [21] applies a statistical model to predict line shadow prices. EPRI [22] has developed a congestion forecasting model that uses sequential Monte Carlo simulation to produce a probabilistic load flow. The EPRI model provides congestion probabilities for transmission lines of interests, but it requires intensive data input to the load flow model.

Li and Bo [23]-[24] examine LMP variation in response to load variation, and they predict the next binding constraint when load is increased. However, the authors also assume

that a particular system growth pattern exists and that load growth at each bus is proportional to this pattern. Most U.S. wholesale power markets operating under LMP are geographically large; hence, distributed loads do not necessarily exhibit proportional growth. Moreover, the authors' approach has not been applied in large-scale power systems where practical issues of limited data availability need to be considered.

In our study [25], a piecewise linear-affine mapping between distributed loads and DC-OPF system variable solutions was identified and applied to forecast congestion and LMPs under the maintained assumption that complete historical information was available regarding the marginality (or not) of generating units and the congestion (or not) of transmission lines. This method is able to give an exact prediction result since it is derived from the core structure of a wholesale power market. However, when applied to the actual forecasting of large-scale wholesale power systems, data requirements become a problem. The needed historical generation capacity data and line flow data are either publicly unavailable on market operator websites or only available with some delay. Consequently, the correct pattern of binding constraints corresponding to any possible future load point is difficult to effectively identify, which in turn prevents the accurate forecasting of system variables.

1.2.2 Transmission Investment for Integrating Renewable Energy

The transmission expansion planning problem has been addressed by a number of researchers from technical point of view. Garces *et.al* proposed a bilevel approach for transmission planners to minimize network cost while facilitating energy trading [26]. A multi-objective framework is developed to handle different stakeholders' interests [27], and

transmission planning models proposed in [28] and [29] take into account the demand uncertainty. Transmission expansion methodologies regarding the uncertainty from large-scale wind farms are presented in [30] and [31]. Sauma and Oren [32] provide an evaluation method for different transmission investments based on equilibrium models with the consideration of interactive generation firms.

These studies focus on solving optimal transmission investment decisions in centralized approaches which are usually undertaken by centralized transmission planners or regulatory bodies. The centralized planning is associated with a FERC approved rate method for the transmission developers, typically the traditional utilities, to recover their costs of investment. A number of rate methods have been examined in the literature. Typically, a postage stamp rate is adopted to recover the fixed transmission cost [33]. Different usage-based methods are also suggested and evaluated by Pan *et. al* [33]. The potential fairness issue in usage-based methods is attempted to resolve using min-max fairness criteria [34]. In addition to the rate structure, Galiana *et.al* proposed a cost allocation methodology based on the principle of equivalent bilateral exchanges. The allocated cost responsibilities are then used to set the rates for different LSEs. Finally, different allocation and rate setting approaches are presented in [35]-[39].

Independent from the centralized planning performed by RTOs such as PJM, research effort has been dedicated to explore market-based transmission planning models which can be considered as decentralized approaches for transmission investment. Roh *et al.* [40] proposed a coordinated transmission and generation planning model which incorporates the characteristics from the centralized and decentralized models. RTO acts as a coordinator rather than a decision maker by providing capacity signals to market participants who

independently decide the investment plans. Research has been conducted on merchant transmission projects, a market-based transmission investment in the current US electricity markets. Joskow and Tirole [41] examined performance attributes associated with merchant transmission models with the consideration of several realistic attributes of electricity markets and transmission networks. Salazar *et al.* [42] identified the most opportunistic time to start a merchant transmission project from an investor point of view. In their continued work [43], they proposed a market-based rate design for recovering merchant transmission investment costs from policy makers' point of view.

The transmission investment model in this dissertation differs from the previous work in that the investment of a market-based transmission project is recovered via a negotiated transmission rate from a RE-GenCo to a TransCo. Negotiation results are derived and provide guidance for market participants in an actual negotiation process. Additionally, the model can be used to develop renewable energy subsidies for policy makers to design market incentives for promoting transmission investment and use of renewable energy resources.

1.3 Contributions of this Dissertation

Transmission is a critical component in power systems. Economic analysis of transmission system is an important task to support the decision making in short-term operation and planning. This dissertation is focused on the development of transmission congestion forecasting tool and transmission investment model for integrating renewable energy. The original contributions are summarized as follows:

1. A congestion forecasting tool based on convex hull techniques

The proposed forecasting algorithm is a novel use of convex hull techniques to enable the short-term forecasting of congestion conditions, prices, and other system variables. The convex hull algorithm and probabilistic inclusion test effectively predict congestion patterns at various operating points. Compared with state-of-the-art structural forecasting models, this new method significantly reduces the forecasting data requirement by using only publicly available data but still achieves a high level of accuracy.

2. A novel concept of system patterns to enhance the forecasting accuracy

The forecasting algorithm proposes the new concept of system patterns as an effective way to take generation and transmission capacity constraints into account. This concept captures the core structure of wholesale power markets and hence permits more accurate forecasting results. The new method exploiting the system pattern concept outperforms traditional statistical forecasting models for large-scale power systems.

3. A negotiation methodology for renewable energy transmission investment based on Nash Bargaining theory

The proposed transmission investment model based on Nash Bargaining approach provides a decentralized methodology for integrating renewable energy. The negotiation methodology takes into account electricity market uncertainties and the intermittent nature of renewable energy. The negotiated results provide guidelines for renewable energy generation and transmission companies in sharing and recovering integration and investment cost.

4. A new approach to evaluate renewable energy subsidy policy

The comparison between negotiation and centralized planning addresses the issue of optimal subsidy policy to produce sufficient incentives for renewable energy investment. The optimal subsidy policy can steer the negotiated solution to a centralized solution that

maximizes the social surplus. The results provide important guidance for policy makers to establish proper renewable energy subsidies.

1.4 Thesis Organization

This research conducts an economic analysis for transmission operation and planning. Specifically for short-term transmission operation, it is intended to provide a congestion and price forecasting tool by analyzing the fundamentals of power markets. For long-term transmission planning, a systematic negotiation methodology among market participants is provided for renewable energy investment incorporating the stochastic nature of renewable resources. The comparison between the negotiation model and centralized planning model is a resource for decision support in policy making of renewable energy subsidies.

Chapter 2 presents a congestion forecasting tool based on the results of [44]. A new short-run congestion forecasting algorithm is proposed based on the concept of system patterns—combinations of status flags for transmission lines and generating units. It is shown that the load space can be divided into convex sets within which system variables can be expressed as linear-affine functions of loads. Congestion forecasting is then transformed into the problem of identifying the correct system pattern. A convex hull algorithm is developed to estimate the convex sets in the load space. A point inclusion test is used to identify the possible system patterns and congestion conditions for a future operating point and a corresponding "sensitivity matrix" is used to forecast LMPs and line shadow prices. Forecasting results based on a NYISO case study demonstrate that the proposed forecasting procedure is highly efficient.

Chapter 3 outlines the research on transmission investment to integrate renewable energy. The negotiation process is analyzed for renewable energy interconnection between a RE-GenCo and a TransCo. Nash Bargaining theory is adopted to determine the transmission investment plans and RE-GenCo's transmission payment. The negotiation methodology as well as its results provides an alternative means to transmission planning for integrating renewable energy. By modifying the included subsidies, the proposed negotiation approach produces results (i.e. transmission plan and rate) mirroring those from a centralized planning model in which the objective is to maximize the overall social surplus. The renewable energy subsidies can be used as an adjusting parameter to steer the investment plan derived from the negotiation towards an optimal plan. This result and comparison provide important guidance to policy makers for determining appropriate renewable energy subsidies.

Chapter 4 provides conclusions and discusses the future research directions.

CHAPTER 2. SHORT-TERM TRANSMISSION CONGESTION FORECASTING

2.1 Introduction

In this chapter, a new algorithm is developed for the short-term forecasting of system variables in wholesale power systems with substantially reduced data requirements. This algorithm permits the derivation of estimated probability distributions for congestion, LMPs, and other DC-OPF system variable solutions in real-time markets and in forward markets with hour-ahead, day-ahead and week-ahead time horizons, conditional on a given commitment-and-line scenario that specifies a set of generating units committed for possible dispatch and a set of transmission lines capable of supporting power flow. Moreover, given suitable availability of historical data, this scenario-conditioned forecasting algorithm can be generalized to a cross-scenario forecasting algorithm by the assignment of probabilities to different commitment-and-line scenarios.

This new forecasting algorithm makes use of two supporting techniques in order to substantially reduce the amount of required data relative to [25]. The first technique is a method developed by Bemporad et al. [45] and Tøndel et al. [46] for dividing the parameter space of a Quadratic-Linear Programming (QLP) problem into convex subsets such that, within each convex subset, the optimal solution values can be expressed as linear-affine functions of the parameters. A similar technique is applied in this study to a QLP DC-OPF problem formulation to show that, conditional on any given commitment-and-line scenario, the load space can be divided into convex subsets within which the optimal DC-OPF system

variable solutions are linear-affine functions of load. Each convex subset corresponds to a unique system pattern, that is, a unique array of flags reflecting a particular pattern of binding minimum or maximum capacity constraints for the committed generating units and available transmission lines specified by the commitment-and-line scenario.

The second technique concerns convex hull determination. Given any collection of points, computational geometry [47] provides algorithms to compute the corresponding convex hull, i.e., the smallest convex set containing these points. Convex hull algorithms have been gaining popularity in the areas of computer graphics, robotics, geographic information systems and so forth. To date, however, they have not been applied in electricity market forecasting. A convex hull algorithm is used in this study to estimate the convex subsets of load space within which DC-OPF solutions are linear-affine functions of load when incomplete historical data prevent their exact determination.

More precisely, the proposed forecasting algorithm generates short-term forecasts for congestion, LMPs, and other power system variables as follows. Let L denote a vector of loads at some possible future operating point corresponding to a particular commitment-and-line scenario S. A convex hull method is first used to estimate the division of load space into convex subsets (system pattern regions), each corresponding to a distinct historically-observed system pattern of binding capacity constraints for the particular committed generating units and available transmission lines specified under S. A probabilistic point inclusion test is next used to calculate the probability that L is associated with each historical system pattern, taking into account the imprecision with which the system pattern regions in load space are estimated. The congestion conditions at L are then probabilistically forecasted using the probability-weighted historical system patterns, and forecasts for LMPs and other

system variables at L are calculated using the linear-affine mapping between load and DC-OPF system variable solutions that corresponds to each probability-weighted historical system pattern.

2.2 Basic Forecasting Problem Formulation

In electricity markets, congestion occurs when the available economical electricity has to be delivered to load "out-of-merit-order" due to transmission limitations. That is, higher-cost generation needs to be dispatched in place of cheaper generation to meet this load in order to avoid overload of transmission lines. In this case, the LMP levels at different nodes separate from each other and from the unconstrained market-clearing price. Therefore, congestion is a critical factor determining the formation of LMP levels.

However, congestion patterns are difficult to anticipate since they are related to the network topology of power systems. Provided perfect information is available, such as network data, load data, and generator bidding data, a market clearing model could be utilized to obtain accurate forecasts of congestion conditions and prices. Nevertheless, two issues arise for this direct forecasting method. First, most market traders do not have direct access to the information that is needed to implement this method; they would have to depend on data published by market operators. Second, the market operators, themselves, would need a high degree of computational speed to carry out the required computations.

As a result, statistical tools have been developed that tackle these two forecasting issues by modeling the statistical correlation between prices and explanatory factors. These statistical tools lack explicit consideration for congestion, partly because no effective approach has been developed to enable these tools to capture and express the effects of

congestion. Ignoring the effects of congestion makes the forecasted prices less reliable and difficult to interpret at operating points with abnormal price behaviors.

Surely it is possible to glean some useful information about future possible congestion conditions based on statistically forecasted LMPs. However, these intuitive insights, based on forecasters' experiences, cannot provide reliable congestion forecasts. From a cause-and-effect point of view, congestion is the cause while LMP is the effect. One cannot infer the cause (congestion) from the effect (LMP) since LMP is not solely driven by congestion. In particular, statistical LMP forecasting tools do not take into account the structural aspects of power markets that fundamentally drive the determination of LMPs: namely, the fact that LMPs are derived as solutions to optimal power flow problems subject to generation capacity and transmission line constraints.

As explained more carefully in Section 2.3.1, the novel concept of a "system pattern" is used in this study to incorporate the structural generation capacity and transmission line aspects that drive congestion outcomes. The forecasting of congestion at a possible future operating point is thus transformed into a problem of estimating the correct system pattern at this operating point. Moreover, the forecasting of prices and other system variables at this operating point can subsequently be undertaken using the particular linear-affine mapping between load and DC-OPF system variable solutions that is associated with this system pattern.

This basic forecasting approach makes three simplifying assumptions. First, it is assumed that the forecasting of system variables at possible future operating points can be conditioned on a particular commitment-and-line scenario, that is, a particular generation commitment (designation of generating units available for dispatch) and a particular network

topology (designation of available transmission lines). Second, it is assumed that a lossless DC-OPF problem formulation is used for the determination of LMPs and other system variables, implying in particular that the loss components of LMPs are neglected. Third, it is assumed that generator supply-offer behaviors are relatively static in the forecasting horizons.

2.3 Basic Forecasting Algorithm Description

2.3.1 System Patterns and System Pattern Regions

At any system operating point, the number of marginal generating units and binding transmission constraints tends to be small compared to the number of nodes, transmission lines, and generating units. For example, in the Midwest Independent System Operator (MISO) region with 36,845 network buses and 5,575 generating units, the number of day-ahead binding constraints is published daily and is typically observed to be less than 20 for an hourly interval [48]. On the other hand, high-cost units such as gas and oil units are more likely to become marginal units during peak hours, the number of which is modest.

Exploiting this important characteristic of power markets, the idea of a *system pattern* is introduced consisting of a vector of flags indicating the marginal status of committed generating units and the congestion status of available transmission lines at any given system operating point; see Table 1. As long as the number of marginal generating units (labeled 0) and the number of congested transmission lines (labeled -1 or 1) are relatively few in number, the number of possible system patterns can be easily handled.

As noted in Section 2.2, the basic congestion forecasting problem can then be transformed into a problem of estimating the correct system pattern for any given possible

future operating point. The congestion forecast is directly obtained once the system pattern is estimated, since the status of transmission lines is part of the system pattern. Moreover, as clarified below in Section 2.3.4, short-term forecasts for prices and other system variables at the operating point can also be obtained making use of this estimated system pattern.

Table 1. Flags used for system patterns

	Generating units			**Transmission lines**		
State	Minimum Capacity	Marginal Unit	Maximum Capacity	Negative Congestion	No Congestion	Positive Congestion
Flag	-1	0	1	-1	0	1

The proposition below provides the theoretical foundation for our proposed forecasting approach. The proposition uses the concept of a *convex polytope* for an n-dimensional Euclidean space R^n, i.e., a region in R^n determined as the intersection of finitely many half-spaces in R^n.

Proposition 1: *Suppose a standard DC-OPF formulation with fixed loads and quadratic generator cost functions is used by a market operator to determine system variable solutions. Then, conditional on any given commitment-and-line scenario S, the load space can be covered by convex polytopes such that: (i) the interior of each convex polytope corresponds to a unique system pattern; and (ii) within the interior of each convex polytope the system variable solutions can be expressed as linear-affine functions of the vector of distributed loads.*

The proof of Proposition 1, originally derived in [44], is outlined in an appendix to this dissertation. The proof starts with the derivation of inequality and equality constraints constructed from the first-order KKT conditions for a DC-OPF problem conditional on a

particular commitment-and-line scenario *S*. The inequality constraints characterize convex polytopes that cover the load space, where the interior of each convex polytope corresponds to a unique system pattern. The convex polytopes constituting the covering of the load space are referred to as *System Pattern Regions (SPRs)* for the fact that the interior of each convex polytope is associated with a unique system pattern.

Within each SPR the equality constraints take the form of linear-affine equations with constant coefficients that describe fixed linear-affine relationships between DC-OPF system variable solutions and the vector of loads. The matrix of coefficients for these linear-affine functions gives the rates of change with regard to real-power dispatch levels for generating units and shadow prices for bus balance and line constraints when loads are perturbed within the region. This matrix is referred to below as the *sensitivity matrix* for this SPR.

Figure 1 provides illustrative depictions of two SPRs, R_1 and R_2, together with their associated linear-affine mappings, when the load space is composed of two-dimensional load vectors $L = (L_1, L_2)$. The symbol P denotes the vector of unit dispatch levels, and the symbol Λ denotes the vector of dual variables. The mappings are characterized by sensitivity matrices (K_1, K_2) and ordinate vectors (K_1^0, K_2^0) that are constant within each SPR, which implies that the DC-OPF solutions for P and Λ can be expressed as fixed linear-affine functions of the load vector L within each SPR.

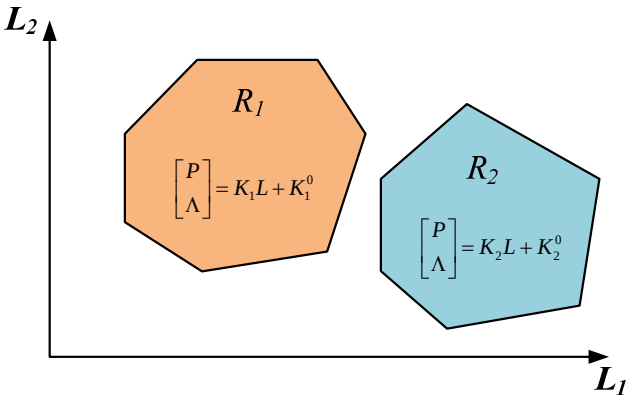

Figure 1. Illustration of two system pattern regions (SPRs) in load space

2.3.2 Convex Hull Estimation of Historical SPRs

In practice, deriving the exact form of the SPRs is difficult due to limited access to most of the required information. This required information includes supply offer data, generating unit capacity data, and transmission limit data.

This lack of information can be overcome by applying a "convex hull algorithm" to historical load data to estimate SPRs. The *convex hull* of a point set *B* is the smallest convex set that contains all the points of *B* [49]. A *convex hull algorithm* is a computational method for computing the convex hull of a set *B*.

Each historical load point corresponding to a particular commitment-and-line scenario *S* can in principle be associated with a distinct system pattern based on corresponding historical data regarding the marginal status of the committed generating units and the congested status of the available transmission lines. The historical SPR corresponding to each such historically identified system pattern can then be estimated by

deriving the convex hull of the collection of all historical load points that have been associated with this system pattern.

This study makes use of the "QuickHull algorithm" to estimate historical SPRs conditional on a given commitment-and-line scenario *S*. The QuickHull algorithm, developed by Barber *et al.* [50], is an iterative procedure for determining all of the points constituting the convex hull of a finite set *B*. At each step, points in *B* that are internal to the convex hull of *B*, and hence not viable as vertices of the convex hull, are identified and eliminated from further consideration. This process continues until no more such points can be found.

An illustrative application of the QuickHull algorithm for a finite planar set *B* is presented in Figure 2. The set *B* is first partitioned into two subsets *B1* and *B2* by a line *lr* connecting a left-most upper point *l* to a right-most lower point *r*, as depicted in in Figure 2(a). More precisely, the points in *B* with the smallest x value are first selected and, from among these points, a point with a largest y value is chosen to be the left-most upper point *l*; similarly for the right-most lower point *r*. For each subset *B1* and *B2*, a point *z* in *B* that is furthest from *lr* is determined and two additional lines are constructed, $\overline{lz}$ from *l* to *z* and $\overline{zr}$ from *z* to *r*; see Figure 2(b). By construction, points of *B* that lie strictly inside the resulting triangle *lzr* are strictly interior to the convex hull of *B* and hence can be eliminated from further consideration. The points on the triangle itself are possible vertex points for the boundary of the convex hull of *B*.

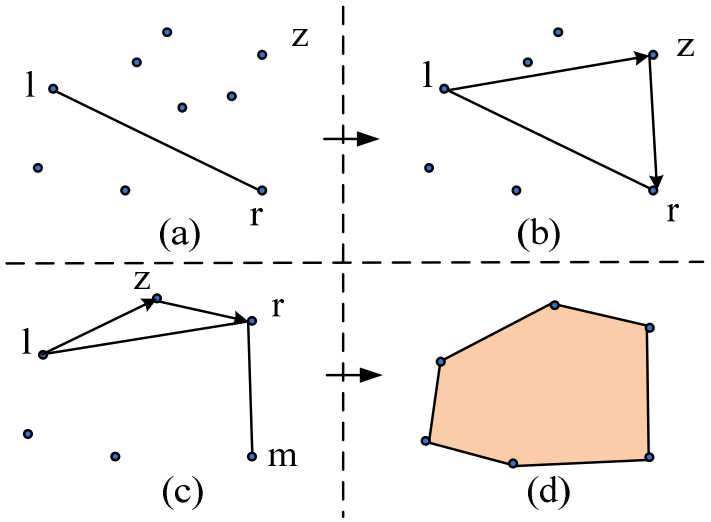

Figure 2. Illustration of the QuickHull algorithm

To continue the recursion, the above procedure is repeated for the reduced subset *BRed* of *B* resulting from this elimination. Specifically, two subsets and associated triangles are formed as before for *BRed* and the points of *BRed* lying within the interiors of the resulting triangles are eliminated. If a triangle ever degenerates to a line, then all the points along the line lie on the boundary of the convex hull of *B* by construction. For example, in Figure 2(c) the endpoints *r* and *m* of the line *rm* both lie on the boundary of the convex hull of *B*.

This process of elimination continues until no additional points to be eliminated can be found. Since *B* is finite, the process is guaranteed to stop in finitely many steps. All the convex hull points for *B* (boundary and interior) can be determined recursively in this manner. The complete convex hull for *B* is depicted in Figure 2(d). By construction, this convex hull is a planar convex polytope.

The main advantage of the QuickHull algorithm relative to other such algorithms is its ability to efficiently handle high-dimensional sets *B* by reducing computational

requirements [51]. The QuickHull algorithm has been widely used in scientific applications and appears to be the algorithm of choice for higher-dimensional convex hull computing [52].

2.3.3 Basic Point Inclusion Test

Suppose the load space has been divided up into estimated SPRs whose interiors correspond to distinct system patterns, conditional on a given commitment-and-line scenario *S*. Consider, now, the task of forecasting congestion conditions at some future operating point a short time into the future for which scenario *S* again obtains. The essence of this forecasting problem is the detection of the correct SPR for this future operating point. If the correct SPR can be detected, then congested conditions can be inferred directly from the corresponding system pattern.

This detection is undertaken in this study by means of a "point inclusion test". The *basic point inclusion test* used in this study is illustrated in Figure 3 for an SPR in a load plane. Recall that each SPR takes the form of a convex polytope, i.e., a region expressable as the intersection of half-spaces; hence each SPR has flat faces with straight edges. Let the normal vectors pointing towards the interior of the SPR be constructed for each edge of the SPR. Now consider the depicted point P_1, and let $\overrightarrow{aP_1}$ denote the vector directed from the vertex a to the point P_1. The dot product between $\overrightarrow{aP_1}$ and each normal vector of each neighboring edge of a is greater than or equal to 0. If this is true for all vertices of the SPR, the point P_1 is judged to be on or inside the SPR. On the other hand, one can see that P_2 is outside the SPR since the dot product of $\overrightarrow{aP_2}$ and the normal vector for the neighboring edge connecting a to b is negative.

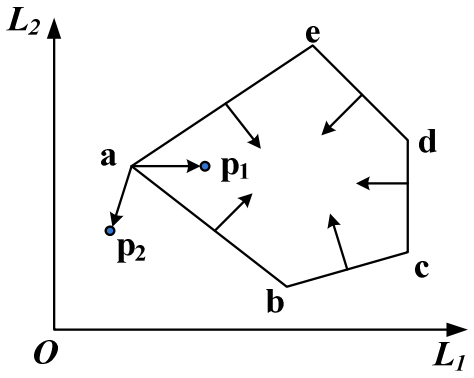

Figure 3. Illustration of the basic point inclusion test for an SPR in a load plane

As will be seen in Section 2.4, practical data-availability issues prevent the use of the basic point inclusion test for the exact determination of the SPR containing any possible future load point *L*. However, given a suitable probabilistic extension of this basic point inclusion test, the probability that any particular SPR contains *L* can be estimated.

2.3.4 Linear-Affine Mapping Procedure

Given sufficient generation and transmission information, each historical load point can be associated with an SPR according to the status of the generating units and transmission lines at the historical operating time. More precisely, given any commitment-and-line scenario *S*, consider the collection of all historically observed load points obtaining under *S*. Let this collection of historical load points be partitioned into subsets corresponding to distinct system patterns for scenario *S*. For each load subset, use the QuickHull algorithm to calculate its convex hull in load space. Each of these convex hulls then constitutes a distinct estimated SPR for scenario *S*. In principal, any future load point corresponding to scenario *S* can then be associated with one of these estimated SPRs by means of the basic

point inclusion test. This association permits the prediction of congestion, prices, and other DC-OPF system variable solutions at this load point.

To see this more clearly, let Y_i^h and L_i^h denote matrices consisting of all historically observed DC-OPF system solution vectors and load vectors corresponding to a particular system pattern *i* for a particular commitment-and-line scenario *S*. Let the SPR in load space corresponding to this system pattern, denoted by R_i, be estimated by the convex hull R_{Ei} of the collection of all of the historically observed load vectors included in L_i^h.

By Proposition 1, the mapping between Y_i^h and L_i^h can be expressed in the linear-affine form

$$Y_i^h = K_i L_i^h + K_i^0 \tag{1}$$

where K_i denotes the sensitivity matrix corresponding to R_i. Normally there will be multiple historical operating points corresponding to any one SPR for a given commitment-and-line scenario *S*. In this case Ordinary Least Squares (OLS) can be applied to **(1)** to obtain estimates $\hat{K}_i$ and $\hat{K}_i^0$ for K_i and K_i^0, as follows:

$$\begin{bmatrix} (\hat{K}_i)^T \\ (\hat{K}_i^0)^T \end{bmatrix} = \left(\mathbf{X}^T\mathbf{X}\right)^{-1}\mathbf{X}^T(\mathbf{Y}_i^h)^T \tag{2}$$

where $\mathbf{X} = [(L_i^h)^T \quad \mathbf{1}]$.

Now let L_i^f denote a possible load vector for a future operating time that has been found to belong to the *estimated* SPR R_{Ei}, as determined from a basic point inclusion test applied to the collection of all historically estimated SPRs corresponding to scenario *S*. Then the forecasted vector Y_i^f of DC-OPF system variable solutions corresponding to L_i^f can be calculated as

$$Y_i^f = \hat{K}_i L_i^f + \hat{K}_i^0 \quad (3)$$

The above linear-affine mapping procedure is modified in Section 2.4 to accommodate some practical issues arising from data incompleteness.

2.4 Extension to Probabilistic Forecasting

Practical data availability issues arise for the implementation of the basic scenario-conditioned forecasting algorithm outlined in Section 2.3. This section discusses how these issues can be addressed by means of a probabilistic extension of this basic algorithm. Throughout this discussion the analysis is assumed to be conditioned on a given commitment-and-line scenario *S*.

2.4.1 Practical Data Availability Issues

The basic scenario-conditioned forecasting algorithm proposed in Section 2.3 assumes that historical data are available regarding binding constraints for all generating units and for transmission lines on an hourly basis. In actuality, however, the marginal status of generating units is either confidential or published with limitations. Moreover, the theoretical load space cannot be fully reflected by the hourly historical load data which represent several realizations and subsets of the complete load space.

Due to these data limitations, in practice the set A indexing hourly binding constraints cannot be completely determined. Consequently, estimates obtained for the SPRs could be biased. The two basic ways in which this bias could arise are illustrated in Figure 4 for a simple two-dimensional load space. Suppose the SPR corresponding to the true binding constraint set A is given by R_A (area 1) in Figure 4.

This true SPR R_A can in principle be determined by applying the basic point inclusion test to every possible future operating point. Suppose, however, that the practically estimated binding constraint set A_{E1} is incomplete; for example, suppose A_{E1} only reflects the status of the most frequently congested lines. Given complete historical load data, the estimated convex hull R_{E1} (area 3) would then have to be larger than the true R_A (area 1) because A_{E1} is smaller (less restrictive) than the true A . In fact, however, the actual estimated convex hull must be based on available historical load data. Since the latter is only a subset of the full load space, the result will be an actual estimated convex hull R_E (area 2) that lies within R_{E1} (area 3). In short, incompleteness of A and incompleteness of the practical load space each separately introduce bias in the estimate for R_A, but in opposing directions.

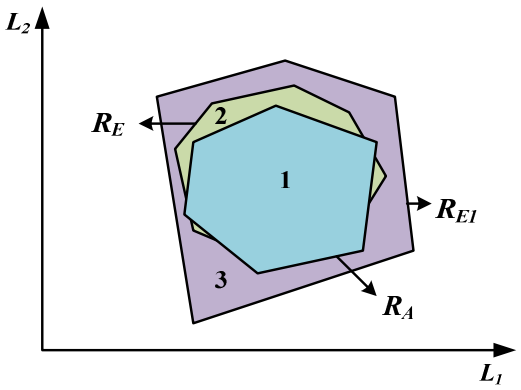

Figure 4. Convex hull estimates for SPRs can be biased

What are the practical implications of this bias for our basic forecasting algorithm? Two possible cases need to be handled, as illustrated in Figure 5.

Case A: Point *r* in Figure 5 lies in the interior of two different estimated SPRs, namely, R_{E1} and R_{E2} corresponding to two distinct system patterns A_1 and A_2. The true SPRs corresponding to A_1 and A_2 are denoted by the shaded regions R_{A1} and R_{A2}, respectively. The

fact that the interiors of the true SPRs do not overlap follows from Proposition 1. However, as explained above, overlap can occur for the interiors of estimated SPRs due to bias.

Case B: Point *t* in Figure 5 is actually in the true SPR R_{A2}. However, point *t* cannot be assigned to either of the estimated SPRs because the bias in these estimates has caused point *t* to lie outside of both of them.

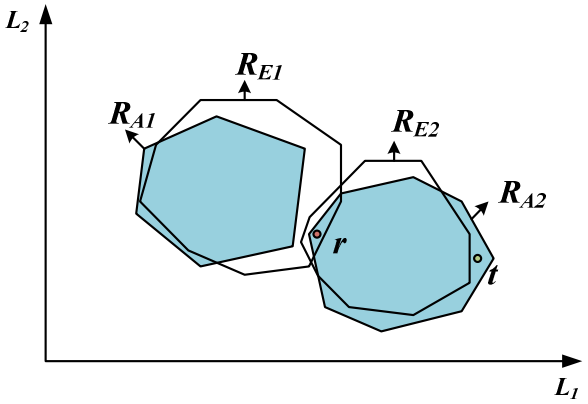

Figure 5. Two possible types of forecast error due to biased SPR estimates

2.4.2 Probabilistic Point Inclusion Test

To mitigate the issues arising from the two types of bias discussed in Section 2.4.1, mean and interval forecasting can be performed for the DC-OPF system variable solutions corresponding to any forecasted future load point L^f. This probabilistic forecasting can be implemented by estimating the probability of each SPR conditional on L^f, which can be characterized as a *probabilistic point inclusion test*.

More precisely, let L^f denote the forecasted load at a future operating point *f*, and let R_i denote any particular SPR *i*. Let the collection of all historically identified SPRs be denoted by R^h, and let *CR* denote the cardinality of R^h. Suppose the probability of occurrence

for any SPR not in R^h is zero. Then the probability that R_i has occurred, given that L^f has been observed, can be expressed as:

$$P(R_i \mid L^f) = \frac{P(L^f \mid R_i)P(R_i)}{\sum_{i \in R^h} P(L^f \mid R_i)P(R_i)} \tag{4}$$

In practice, the various terms in (4) have to be estimated. In this study it will be assumed that the prior probability $P(R_i)$ is an empirical prior estimated by the historical frequency of R_i: namely, the number of times in the past that R_i has been observed to occur divided by the total number of all past SPR observations.

The term $P(L^f \mid R_i)$ in (4) represents the probability of observing the load point L^f given that the true SPR is R_i. Intuitively, this probability should be a decreasing function of the distance between L^f and R_i. Therefore, this probability is estimated in this study as follows:

$$\hat{P}(L^f \mid R_i) = \frac{(1 - D_i / TD)^\gamma}{\sum_{i \in R^h} (1 - D_i / TD)^\gamma} \tag{5}$$

In (5) the term D_i denotes the (Euclidean) distance between L^f and R_i, and TD denotes the total distance calculated as the sum of the distances between L^f and each SPR in R^h. The *normalization parameter* γ in (5) can be adjusted to obtain an appropriate conditional probability measure, possibly by using historical data as training cases. A specification $\gamma = 0$ results in a uniform conditional probability (5) for L^f: namely, 1 divided by the cardinality CR of R^h. In this case (5) is independent of the distance measures D_i. Alternatively, a specification $\gamma = 1$ implies the conditional probability (5) is derived from a linear normalization, while $\gamma = 2$ corresponds to a quadratic normalization. As will be shown

below, the quadratic normalization form of the conditional probability (5) results in good forecasts for our NYISO case study.

Mean forecasts for the DC-OPF system variable solutions at the operating point *f* with forecasted load point L^f can then be obtained using the estimated form for the conditional probability assessments (4), denoted by P_i^f for short. Let Y_i^f denote the forecasted DC-OPF system variable solution vector corresponding to any historical SPR R_i in R^h. The mean forecast $\bar{Y}^f$ can then be calculated as

$$\bar{Y}^f = \sum_{i \in R^h} P_i^f Y_i^f \tag{6}$$

A forecaster might also be interested in calculating upper and lower bounds for the DC-OPF system variable solutions calculated with respect to the most likely SPRs. Let *nmp* denote the forecaster's desired cut-off number of most probable SPRs, and let *MP* represent the subset of R^h that contains these *nmp* most probable SPRs. Then the upper bound UB^f and lower bound LB^f for each forecasted DC-OPF system variable solution can be determined over the set of SPRs in *MP*. As a measure of dispersion, the forecaster can further consider the *coverage probability CP*, defined to be the summation of the probability assessments (4) for the *nmp* most probable SPRs.

Finally, another alternative might be for the forecaster to consider mean forecasts calculated using the *nmp* most probable SPRs, i.e. the subset *MP* of R^h. For example, a forecaster could choose *nmp*=1, which would result in a point forecast for the DC-OPF system variable solutions based on a single most likely SPR R_i in R^h as determined from the estimated form of the conditional probability assessments (4).

2.4.3 Probabilistic Forecasting Algorithm

Taking into account the practical data issues addressed in Sections 2.4.1and 2.4.2, our proposed probabilistic forecasting algorithm proceeds in four steps, as follows:

Step 1: Perform historical data processing to identify historical system patterns. Use the QuickHull algorithm to estimate historical SPRs as convex hulls of historically observed load points corresponding to distinct historical system patterns.

Step 2: For each historical SPR estimated in Step 1, a linear-affine mapping between load vectors and DC-OPF system variable solution vectors is derived using historical load and system variable data. The system variable solution vectors include real-power dispatch levels and dual variables for nodal balance and transmission line constraints. The linear-affine mapping is characterized by a sensitivity matrix and an ordinate vector.

Step 3: For any possible load point L^f in the near future for which system variable forecasts are desired, a probabilistic point inclusion test is performed. More precisely, the estimated form of the conditional probability distribution (4) is used to estimate the probability that L^f lies in each of the historical SPRs identified in Step 1.

Step 4: The results from Steps 1-3 are used to generate probabilistic forecasts at the future possible operating point L^f for generation capacity and transmission congestion conditions (system patterns) as well as for DC-OPF system variable solutions for dispatch levels and dual variables (including LMPs). For example, these probabilistic forecasts could take the form of mean and interval forecasts, or they could be point forecasts based on a most probable SPR.

2.5 Five-Bus System: Basic Forecasting

The input data file for the 5-bus test case included in the download of the AMES Wholesale Power Market Test Bed [53] is used below to illustrate basic forecasting algorithm outlined in Section 2.3. As depicted in Figure 6, this 5-bus test case has six transmission lines (TL1-TL6), five generation units (G1-G5), and three load-serving entities (LSE 1-LSE 3).

The AMES test bed implements a wholesale power market operating over a transmission network with congestion managed by LMP [54]. Profit-seeking generation units in AMES are able to learn over time how to report their supply offers based on their past profit outcomes. In this study, however, it is assumed that each generation unit reports its true cost and capacity attributes to the ISO each day for the day-ahead energy market.

The load data for our 5-bus case study are scaled-down time-varying loads derived from load data available at the MISO website [55]. Using this load data, AMES was run for 365 simulated days in order to determine historical system patterns s. The sensitivity matrix and ordinate vector for each of these patterns was then calculated. System pattern determination and system variable prediction were carried out for various possible distributed load patterns. These steps are explained more carefully in the following subsections.

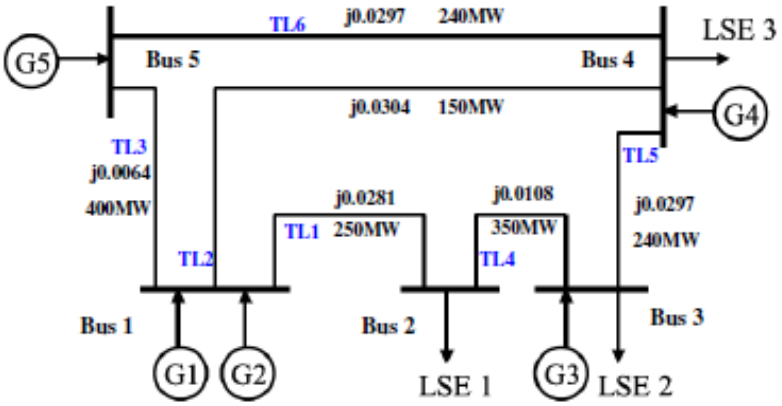

Figure 6. 5-bus network

2.5.1 Historical System Patterns and the Corresponding Sensitivity Matrices

Nine system patterns were identified from the AMES output obtained from the 365 simulated days using a year of scaled-down MISO load data. The four most frequently observed system patterns are displayed in Table 2.

Table 2. The four most frequent historical system patterns for the 5-bus system

Pattern	G1	G2	G3	G4	G5	TL1	TL2	TL3	TL4	TL5	TL6
S1	1	0	-1	-1	0	0	0	0	0	0	0
S2	0	0	0	-1	0	1	0	0	0	0	0
S3	1	0	0	-1	0	1	0	0	0	0	0
S4	1	0	-1	-1	0	1	0	0	0	0	0

The sensitivity matrix and ordinate vector for each of the nine historical system patterns were then estimated making use of actual system operating points observed for each historical system pattern. To illustrate, we compute the sensitivity matrix and ordinate vector for the dispatch level of generation unit G1 in system pattern S4. Specifically, using four

historically observed operating points t = 1,…,4 associated with system pattern S4, a set of four linear equations was determined as follows:

$$P_1^1 = J_{11}^{P4} 4L_1^1 + J_{12}^{P4} L_2^1 + J_{13}^{P4} L_3^1 + O_1^{P4} \quad (7)$$

$$P_1^2 = J_{11}^{P4} 4L_1^2 + J_{12}^{P4} L_2^2 + J_{13}^{P4} L_3^2 + O_1^{P4} \quad (8)$$

$$P_1^3 = J_{11}^{P4} 4L_1^3 + J_{12}^{P4} L_2^3 + J_{13}^{P4} L_3^3 + O_1^{P4} \quad (9)$$

$$P_1^4 = J_{11}^{P4} 4L_1^4 + J_{12}^{P4} L_2^4 + J_{13}^{P4} L_3^4 + O_1^{P4} \quad (10)$$

Here P_1^t denotes the dispatch level of G1 at operating point t and L_j^t denotes the load level of LSE j at operating point t. These four equations determine solution values for the four unknown variables $J_{11}^{P4}, J_{12}^{P4}, J_{13}^{P4}$ and O_1^{P4}. The superscript "P4" represents the dispatch level P in system pattern S4. The subscript "11" denotes the dispatch level of G1 with respect to load level of LSE 1. The first three solution values determine one row of the block matrix J^{P4}, hence also one row of the sensitivity matrix J^4 for system pattern S4. The last solution value determines one element of $\bar{O}^{P4}$, hence one element of the ordinate vector $\bar{O}^4$ for system pattern S4. Other rows and elements can be similarly computed. The sensitivity matrix and ordinate vector for S4 are partially shown in Table 3.

2.5.2 Predicting System Pattern, Congestion and System Variables

Now suppose that a certain distributed load pattern is forecasted for the near future. For example, suppose the forecasted loads for buses 1 through 3 in a particular hour H are L1 = 245.50MW, L2 = 211.64MW, and L3 = 170.17MW. An iterative assume-check procedure can then be undertaken to determine which system pattern corresponds to these forecasted load conditions. Since complete information is available for prediction, the correct system pattern can be found precisely. In this five bus case, the correct system pattern is found to be

S3. LMP and congestion predictions generated for these forecasted loads under system pattern S3 are reported in Table 4, along with the actual LMPs and congestion resulting under this load condition.

Table 3. Sensitivity matrix and ordinate vector for system pattern S4 (partially shown)

O^{LMP}	J^{LMP}
$\begin{bmatrix} 23.83 \\ -3400.00 \\ -2729.20 \\ -994.43 \\ -52.79 \end{bmatrix}$	$\begin{bmatrix} -0.02 & -0.03 & 0.01 \\ 8.74 & 7.12 & 2.35 \\ 7.02 & 5.72 & 1.89 \\ 2.59 & 2.09 & 0.71 \\ -0.17 & 0.15 & 0.05 \end{bmatrix}$
O^{P}	J^{P}
$\begin{bmatrix} 110 \\ 6679.66 \\ 0 \\ 0 \\ -6679.30 \end{bmatrix}$	$\begin{bmatrix} 0 & 0 & 0 \\ -17.21 & -13.89 & -4.23 \\ 0 & 0 & 0 \\ 0 & 0 & 0 \\ 17.92 & 14.68 & 5.14 \end{bmatrix}$
O^{F}	J^{F}
$\begin{bmatrix} 250.00 \\ 601.57 \\ 5938.09 \\ 250.00 \\ 208.97 \\ 741.26 \end{bmatrix}$	$\begin{bmatrix} 0 & 0 & 0 \\ -1.43 & -1.05 & -0.03 \\ -15.78 & -12.87 & -4.20 \\ -1.0 & 0 & 0 \\ -0.89 & -0.92 & 0.03 \\ -2.14 & -1.84 & -0.94 \end{bmatrix}$

Table 4. LMP and line congestion predictions under S3

LMPS	**LMP1**	**LMP2**	**LMP3**	**LMP4**	**LMP5**
Predicted	15.14	29.50	26.79	19.29	15.84
Actual	15.12	29.49	26.77	19.28	15.86
Congested lines		**Predicted: TL1**		**Actual: TL1**	

The proposed approach is also tested for the prediction of LMPs and line flows over successive hours. Figure 7 and Figure 8 display the predicted and actual values for the power flow on line TL1 and the LMP at bus 2 for all 24 hours of the simulated day 363. As seen, the predicted values are nearly coincident with the actual values, differing only by small computational round-off and truncation errors.

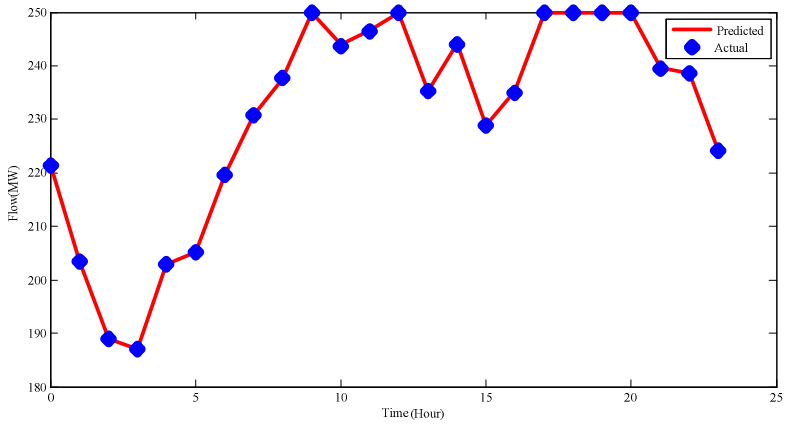

Figure 7. Predicted hourly power flow on line TL1 during day 363

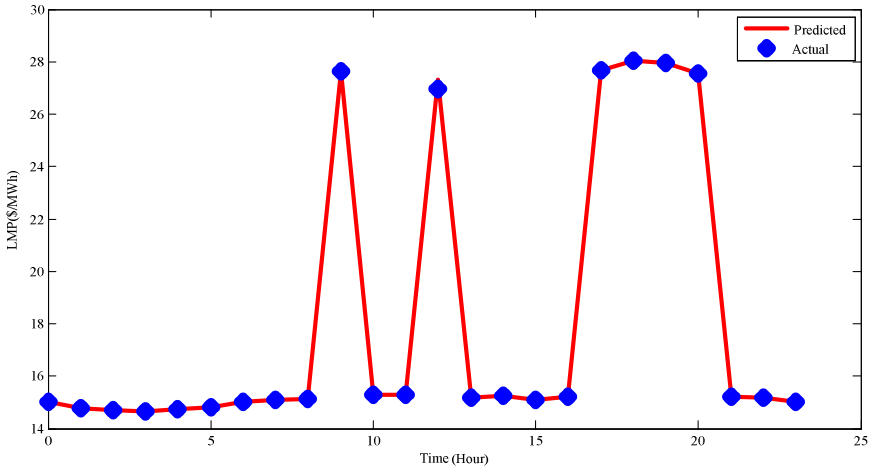

Figure 8. Predicted LMP at bus 2 during day 363

2.6 NYISO Case Study: Probabilistic Forecasting

2.6.1 Case Study Overview

A case study using NYISO 2007 data is reported in this section for the probabilistic scenario-conditioned forecasting algorithm presented in Section 2.4. NYISO has a footprint covering 11 load zones [56]. Short-term zonal load forecasting data and binding constraints data are available at the NYISO website [57].

This forecasting algorithm is applicable for power markets using either nodal or zonal LMP pricing, since Proposition 1 does not rule out either form of pricing. However, NYISO's website [57] only posts daily zonal load data for its 11 load zones, which makes it impossible to forecast prices down to each node. In addition, historical NYISO price data reveal the similarity of LMPs within some of these 11 load zones, hence the negligibility of inter-zonal congestion between these zones. For this reason, to reduce our computational burden without any significant loss of information, we chose to reduce the original 11 load zones for the NYISO to 8 load zones by combining Zone Millwood with Dunwoodie, and Zone West and Genesee with Central.

The top 25 most frequently congested high-voltage transmission lines during 2007 for the NYSIO day-ahead market are studied in [58]. The focus of our case study is on the five most frequently congested high-voltage transmission lines during 2007, specifically, DUNWODIE 345 SHORE RD 345 1 **(D-S)**, CENTRAL EAST-VC **(C-V)**, PLSNTVLY 345 LEEDS 345 1 **(P-L)**, WEST CENTRAL **(W-C)**, SPRNBRK 345 EGRDNCTR 345 1 **(S-E)**. Since the marginal status of generating units is not available from the NYISO, the

conditioning scenario for this empirical study is taken to be the availability of these five lines. System patterns are thus equivalent to congestion patterns for these five lines.

Regarding time period, we selected 12 test days consisting of the last day of each month in 2007. The 24 operating hours starting from 0:00 for each test day were treated as future operating points. Forecasted load data at these hours were used to identify system patterns and to generate system variable forecasts. These forecasted results were then compared with actual realizations to evaluate the performance of our algorithm. Due to space limitations, graphical illustrations are presented only for January 31st and February 28th; numerical results for the last days of other months are given in tables.

All calculations for this case study were implemented using Matlab 7.8 on an Intel Core 2 PC with 3.0GHz CPU. The computational time for each daily forecast was about 2 minutes.

2.6.2 Implementation of Probabilistic Forecasting

Historical price and load data were first processed to identify historical system patterns and SPRs, which is Step 1 of our probabilistic forecasting algorithm. Sorted by congestion patterns, about 19 to 30 historical system patterns (hence SPRs) were found for each forecasted day. For example, the four most frequently observed congestion patterns for January 31st are shown in Table 5. System patterns for other days are categorized similarly.

Step 2 of our algorithm was then carried out. Specifically, the sensitivity matrix and ordinate vector for each historical SPR were estimated by ordinary least squares, making use of the actual system operating points observed for each historical system pattern.

Table 5. Four most frequent historical congestion patterns for 01/31/2007

Pattern	D-S	C-V	P-L	S-C	S-E
P1	1	0	0	0	0
P2	0	0	0	0	0
P3	1	1	0	0	0
P4	1	1	0	1	0

In Step 3, forecasted load data for the 24 operating hours of each test day were then treated as possible future load points. For each of the latter points, the probabilistic point inclusion test detailed in Section 2.4.2 was used to assign estimated conditional probability assessments (4) giving the probability that this future load point was contained within each historical SPR. In these Step 3 calculations, we first evaluated the forecasting performance of three values (0, 1, and 2) for the normalization parameter γ in (5) on the basis of historical data. The specification $\gamma = 2$ gave the best forecast results for most historical days; hence, this value was chosen to forecast system variables for the future load points.

Finally, in Step 4 the results of Steps 1-3 above were used to generate probabilistic forecasts in the form of mean and interval forecasts. For the mean forecasts, *nmp* was set equal to the cardinality *CR* of R^h. For the interval forecasts, *nmp* was set equal to 4.

For the interval forecasts, the size of *nmp* (i.e. the cut-off number of most probable SPRs) depends on the forecaster's desired trade-off between accuracy and precision. A larger *nmp* tends to increase forecasting accuracy, in the sense that there is a better chance the correct SPR will be among the considered SPRs. On the other hand, the precision of any resulting mean forecast is correspondingly reduced (i.e., the variance of the forecasts across the considered SPRs is increased). In the current study, the specification *nmp*=4 is used for

interval forecasts because it results in good precision without significant loss of coverage probability.

2.6.3 Congestion Pattern Forecasts

Table 6 reports the four most probable hourly congestion patterns, along with their associated estimated conditional probabilities and coverage probability *CP* (based on *nmp*=4), for every fifth hour of January 31st, 2007, starting from hour 0:00. Actual congestion patterns corresponding to each reported hour are highlighted in gray. As seen, for the reported hours the actual congestion pattern is always included among the forecasted congestion patterns and has the highest estimated conditional probability. For future reference, note also that the first entry of the actual congestion pattern, corresponding to transmission line D-S, is always 1. This indicates that D-S is frequently congested.

The multiple forecasted congestion patterns associated with each reported hour in Table 6 represent several credible congestion scenarios that could occur in the future. If a forecaster desires to derive one forecast for the future congestion pattern, an intuitively reasonable option would be to select a forecasted congestion pattern that has the highest associated conditional probability (4). As observed in Table 6, for the case study at hand this approach would result in the correct prediction of the actual congestion pattern for each reported hour. In general, however, more reliable forecasts for system conditions and DC-OPF system variable solutions would be obtained by making fuller use of the conditional probability assessments (4) to form mean forecasts and interval forecasts.

Table 6. Forecasted congestion patterns versus the actual pattern on 01/31/2007

Time	Forecasted	Probabilities	CP	Actual
0:00	1 0 0 0 0	0.3632	0.9541	1 0 0 0 0
	0 0 0 0 0	0.2411		
	1 1 0 0 0	0.2066		
	1 1 0 1 0	0.1432		
5:00	1 0 0 0 0	0.3451	0.9398	1 0 0 0 0
	0 0 0 0 0	0.2043		
	1 1 0 0 0	0.2418		
	1 1 0 1 0	0.1486		
10:00	1 0 0 0 0	0.4237	0.9426	1 0 0 0 0
	0 0 -1 0 0	0.0236		
	1 1 0 0 0	0.3654		
	1 1 0 1 0	0.1299		
15:00	1 0 0 0 0	0.3661	0.9452	1 1 0 0 0
	0 0 -1 0 0	0.0271		
	1 1 0 0 0	0.4243		
	1 1 0 1 0	0.1277		
20:00	1 0 0 0 0	0.4247	0.9435	1 0 0 0 0
	0 0 0 0 0	0.0244		
	1 1 0 0 0	0.3612		
	1 1 0 1 0	0.1332		

2.6.4 Mean Forecasts for LMPs

One of the benefits of congestion forecasting is to enable the more precise prediction of LMPs for market operators and traders in their short-term decision making. Forecasted and actual LMPs for Zone Central on Jan 31st and Feb 28th are shown in and Figure 9. *Root Mean Squared Error (RMSE)* and *Mean Absolute Percentage Error (MAPE)* [11] are used as measures of forecast accuracy:

$$\text{RMSE} = \sqrt{\frac{1}{24}\sum_{i=1}^{24}(LMP_i^{actual} - LMP_i^{forecast})^2} \tag{11}$$

$$\text{MAPE} = \frac{1}{24}\sum_{i=1}^{24}\frac{|LMP_i^{acutal} - LMP_i^{forecast}|}{LMP_i^{actual}} \tag{12}$$

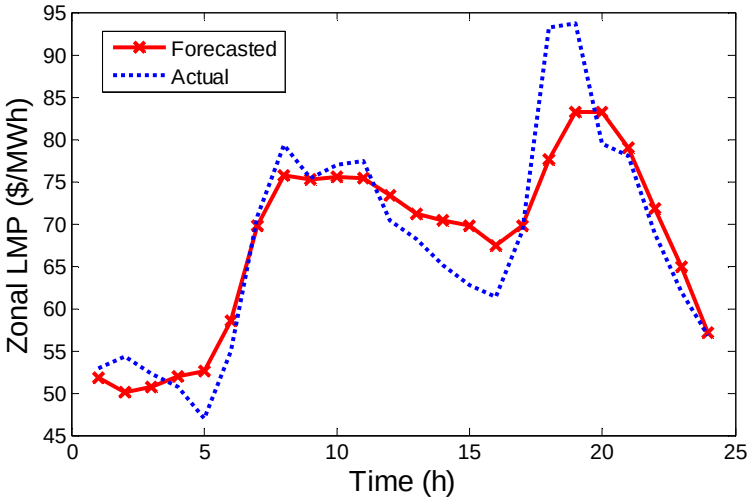

Figure 9. Actual versus mean LMP forecasts for Zone Central on 01/31/2007

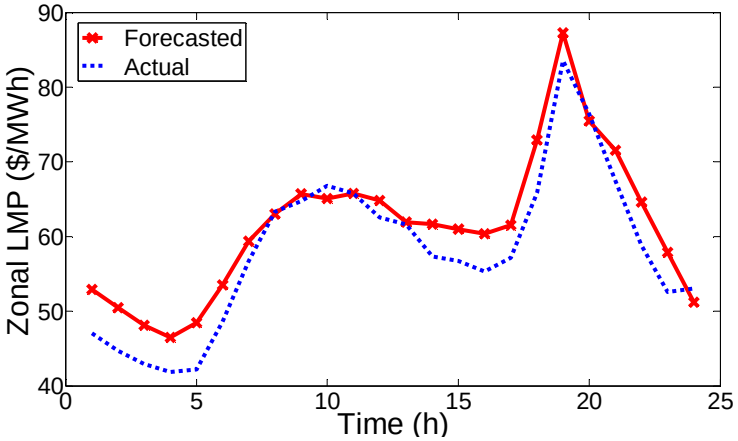

Figure 10. Actual versus mean LMP forecasts for Zone Central on 02/28/2007

Table 7 reports the RMSE and MAPE obtained using our probabilistic forecasting algorithm for each of our 12 test days. Corresponding forecast results obtained using a well-known statistical model – the Generalized Autoregressive Conditional Heteroskedasticity (GARCH) model [10]– are also shown for comparison. As seen, except for the slightly smaller MAPE value attained in February using GARCH, our forecasting algorithm outperforms GARCH in the sense that smaller RMSE and MAPE values are obtained.

Table 7. RMSE and MAPE values for the twelve test days

Day	RMSE		MAPE	
Model	Proposed Alg.	GARCH	Proposed Alg.	GARCH
01/31/2007	5.026	8.689	0.0525	0.0902
02/28/2007	3.393	4.465	0.0472	0.0384
03/31/2007	4.029	7.094	0.0677	0.0727
04/30/2007	4.853	8.297	0.0535	0.1005
05/31/2007	7.401	14.741	0.0934	0.1198
06/30/2007	3.439	13.359	0.0679	0.1485
07/31/2007	3.941	11.623	0.0530	0.1082
08/31/2007	4.076	5.913	0.0671	0.0781
09/30/2007	3.249	6.636	0.0603	0.0862
10/31/2007	4.135	8.561	0.0638	0.1176
11/30/2007	6.476	7.208	0.0770	0.0855
12/31/2007	7.051	14.185	0.0903	0.1435

2.6.5 Interval Forecasts for Line Shadow Prices and LMPs

Interval forecasting is recommended over mean forecasting for line shadow prices. As clarified below, interval forecasting is more informative than mean forecasting for line shadow prices because the underlying attribute of interest (negative-direction, zero, or positive-direction congestion) is measured by a discretely-valued indicator (-1, 0, or 1).

Hourly upper-bound and lower-bound interval forecasts for the line shadow prices on line D-S on January 31st and Feb 28th are shown in Figure 11and Figure 12 along with actual

line shadow prices for comparison. As seen, the actual line shadow prices for most hours fall within the forecasted intervals.

To better interpret these findings, consider the Table 6 results which forecast that line D-S (the first congestion pattern entry) will be either congested or not during hour 20 with varying probabilities. If congestion is forecasted, it is in the positive direction (+1); and, from Figure 11, the line shadow price is estimated to be about $60/MWh. On the other hand, if no congestion is forecasted (0), then from Figure 11 the line shadow price is estimated to be $0/MWh.

One final point for interval forecasts for line shadow prices is important to note. For lines for which no congestion occurs in any of the reported congestion patterns (e.g., line S-E in Table 6), the corresponding upper and lower bounds for the forecasted line shadow price interval will both be zero, indicating zero congestion.

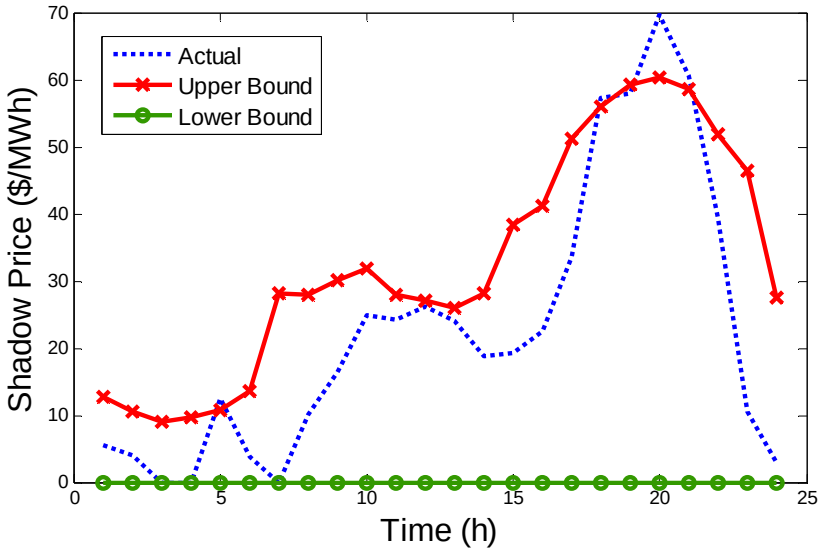

Figure 11. Actual versus interval D-S line shadow price forecasts on 01/31/2007

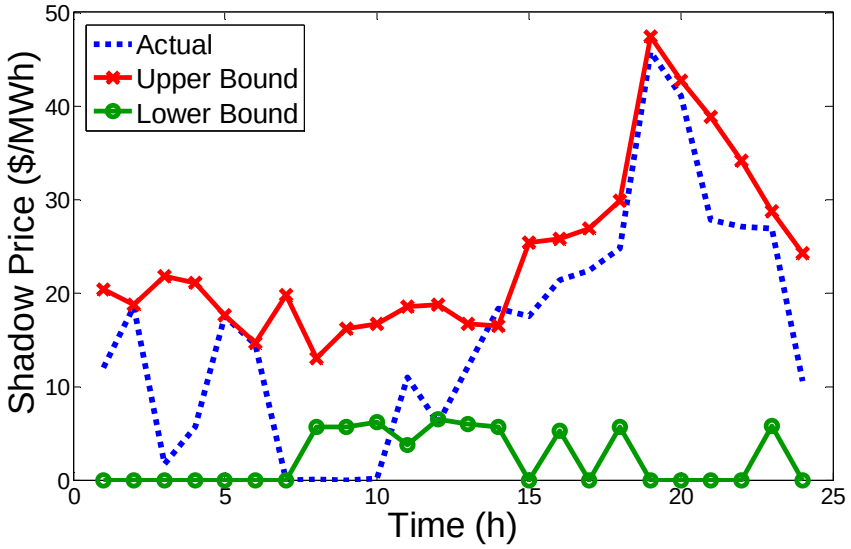

Figure 12. Actual versus interval D-S line shadow price forecasts on 02/28/2007

Interval forecasts for Zone Central LMPs on January 31st and February 28th are shown in Figure 13 and Figure 14 along with actual LMP values for comparison. For most hours the actual LMP values fall within the upper and lower bounds of the forecasted intervals.

The interval forecasting performance for line shadow prices and zonal LMPs is measured using the accuracy-informativeness tradeoff model developed in [59]. The *statistical loss function LOSS* is defined to be

$$LOSS = \frac{|y-m|}{g} + \delta ln(g) \tag{13}$$

In (13), y denotes the actual value, m denotes the midpoint of the forecasted interval, and $ln(g)$ denotes the natural logarithm of the width g of the forecasted interval. Also, δ determines the tradeoff between accuracy (the first term) and informativeness (the second term); in this case study δ is set to 1. Note that a smaller *LOSS* indicates better performance for interval forecasting.

Table 8 gives the *LOSS* values for the interval forecasts obtained for line shadow price and zonal LMPs using our probabilistic forecasting algorithm versus the forecasts obtained using a statistical GARCH model. As seen, our probabilistic forecasting algorithm results in uniformly lower *LOSS* values than GARCH, indicating a better forecasting performance.

A possible explanation for this performance difference is that GARCH has difficulty handling the volatility of line shadow prices, which can abruptly change from 0 to large non-zero values. In contrast, our probabilistic forecasting algorithm captures the physical meaning of these line shadow prices and this facilitates better forecasting.

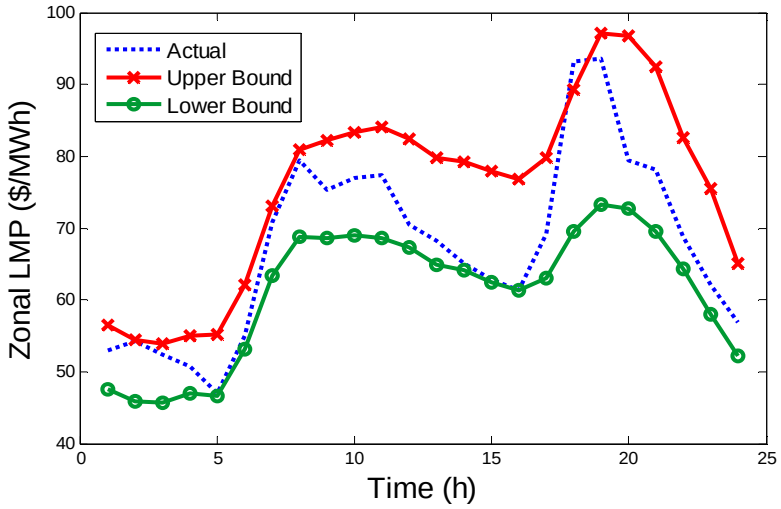

Figure 13. Actual versus interval LMP forecasts for Zone Central on 01/31/2007

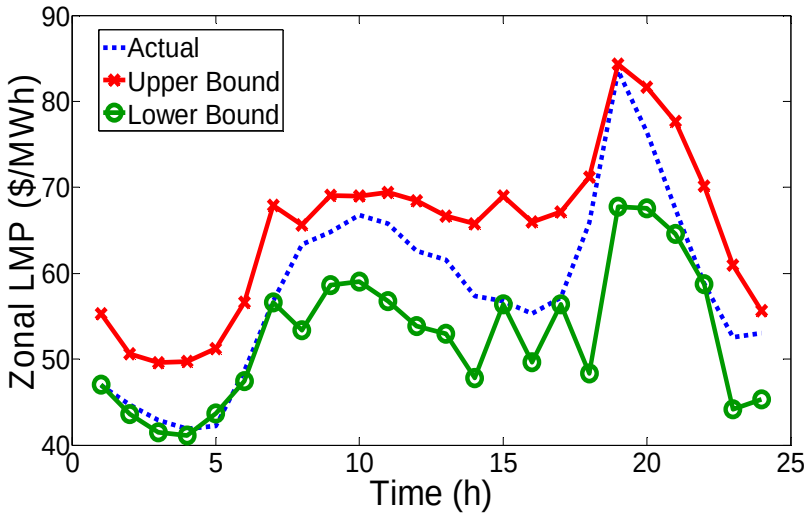

Figure 14. Actual versus interval LMP forecasts for Zone Central on 02/28/2007

Table 8. Loss function values as a measure of interval forecasting performance

Day	**Shadow Price Forecasting**		**LMP Forecasting**	
Model	Proposed Alg.	GARCH	Proposed Alg.	GARCH
01/31/2007	3.824	4.063	2.896	4.196
02/28/2007	3.729	3.977	2.835	3.649
03/31/2007	3.236	3.672	2.574	3.633
04/30/2007	3.398	3.778	3.133	4.164
05/31/2007	3.493	4.187	3.421	4.032
06/30/2007	3.838	3.897	3.365	4.425
07/31/2007	2.726	3.350	2.839	4.892
08/31/2007	2.916	3.352	2.787	3.624
09/30/2007	3.140	3.567	2.245	3.965
10/31/2007	2.825	3.335	2.725	3.799
11/30/2007	3.256	3.738	3.088	3.537
12/31/2007	3.481	3.962	3.164	3.919

In this study we observed that, in some months (January, May, November, and December), the peak-hour LMPs and line shadow prices were difficult to forecast with precision. This phenomenon could possibly be due to changes in the generating unit commitment pattern or in the transmission network topology over the forecast horizon. To enhance peak-hour forecasting results, more careful collection of historical data might be needed to ensure that these historical data correspond to the same commitment-and-line scenario as the forecasted point. Alternatively, as discussed in the following Section 2.7, an extended cross-scenario forecast study could be attempted.

2.7 Extension to Cross-Scenario Forecasting

To this point, the forecasting algorithm developed in this study has been conditioned on a given commitment-and-line scenario *S* specifying a particular generating unit commitment pattern and a particular transmission network topology. One interpretation of *S* is that it represents anticipated conditions at a future operating point for which forecasts are desired. Another interpretation of *S* is that it represents a possible future system contingency (e.g., an N-1 outage scenario) under consideration in a contingency planning study.

A possibly useful extension of this algorithm would be to assign probabilities to distinct scenarios, thus permitting the probabilistic cross-scenario blending of forecasts. These scenarios could be characterized not only on the basis of system patterns, i.e., generating unit commitments and transmission network topology, but also on the basis of a variety of other types of contingencies.

As illustrated in Figure 15, for any future operating point whose system conditions need to be forecasted, the corresponding generating unit commitment, transmission network

topology, and other contingencies could be projected with some probabilities. In each of these projected scenarios, our scenario-conditioned forecasting algorithm could be applied to estimate congestion, LMPs, and other system variables. The final forecast for any system variable of interest could then be the expected value of this system variable calculated across all projected scenarios.

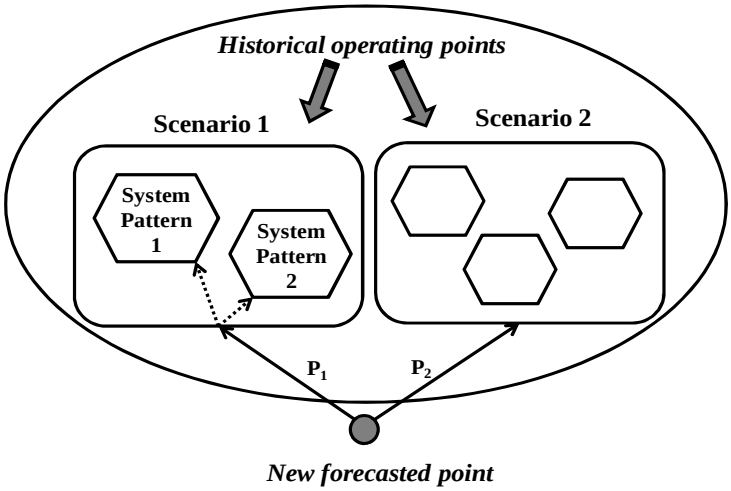

Figure 15. Scenario-conditioned and cross-scenario forecasting

CHAPTER 3. TRANSMISSION INVESTMENT FOR INTEGRATING RENEWABLE ENERGY

3.1 Introduction

In this chapter, a method is proposed to support the negotiation process for renewable energy integration between a Renewable Energy (RE) Generation Company (RE-GenCo) and a Transmission Company (TransCo). The process begins with a prudent development of transmission plans by the two companies, taking into consideration the intermittency of renewable energy such as wind generation. Then the payment from the RE-GenCo to the TransCo is negotiated. If the payment is low, the TransCo may not fully recover its investment; if the payment is high, the RE-GenCo is not profitable. Hence the parties could fail to reach an agreement. Note that this study can also be extended to include a LSE who can contract to purchase a certain amount of renewable energy.

Nash Bargaining theory is applied to determine the transmission investment plans and RE-GenCo's transmission payment. The Nash bargaining solution gives a fair and efficient utility allocation for the two companies. The negotiation methodology as well as its results provides guidelines to transmission investors for integrating renewable energy under uncertainties. The negotiation is then compared with a centralized planning model to evaluate renewable energy subsides. The comparison shed light to policy makers on designing proper renewable energy subsidies.

3.2 Nomenclature

Indices and sets:

n	Index for buses
s	Index for scenarios
t	Index for subperiods
i	Index for generators
j	Index for loads
b	Index for supply or bid blocks
k	Index for transmission lines
$o(k)$	Sending-end of transmission line k
$r(k)$	Receiving-end of transmission line k
R	Index for the bus where renewable generation will be invested
I_r	Index for the renewable generator invested by the RE-GenCo
Ω_N	Set of all system buses
Ω_T	Set of all subperiods
Ω_S	Set of all scenarios
Ω_n^G	Set of generators at Bus n
Ω_n^L	Set of loads at Bus n
Ω_i^b	Set of blocks of Generator i
Ω_j^b	Set of blocks of Load j
Ω^{TG}	Set of traditional generators
Ω^{RG}	Set of renewable generators
Ω^{ET}	Set of existing transmission lines
Ω^{CT}	Set of candidate transmission lines
Ω^G	Set of all system generators
Ω^L	Set of all system loads

Parameters:

D_t	Duration of subperiod *t*
λ_{ib}^{G}	Offer price of the *b*th block by the *i*th generator
λ_{jb}^{L}	Bid price of the *b*th block by the *j*th load
ICT_k	Annualized investment cost of transmission line *k*
$\overline{P}_{ib}^{G}$	Size of the *b*th block for the *i*th generator
$\overline{P}_{jb}^{L}$	Size of the *b*th block for the *j*th load
$\overline{P}_{ibts}^{R}$	Size of the *b*th block for the *i*th renewable generator at subperiod *t* in scenario *s*
$\overline{F}_k$	Transmission capacity of line *k*
x_k	Transmission reactance of line *k*
SUB	Parameter of renewable energy subsidies
IC_{RG}	Annualized investment cost of renewable generation
d_{RG}	Threat point of the RE-GenCo
d_T	Threat point of the TransCo
FP	Renewable energy contract price ($/MWh) for RE-GenCo

Decision variables:

P_{ibts}^{G}	Electricity produced by the *b*th block of *i*th generator at subperiod *t* in scenario *s*.
Y_k	Electricity consumed by the *b*th block of *j*th load at subperiod *t* in scenario *s*.
λ	Negotiated payment from the RE-GenCo to the TransCo.
F_{kts}	Power flow of transmission line *k* at subperiod *t* in scenario *s*.
LMP_{nts}	LMP of Bus *n* at subperiod *t* in scenario *s*.

3.3 Problem Formulation

3.3.1 Overview

This section describes the negotiation process between a RE-GenCo and a TransCo. Assuming that a RE-GenCo has decided to invest in a RE project at a remote location, the

RE-GenCo can pay a construction company to build the interconnection transmission if, in the business case, the RE-GenCo can demonstrate with certainty that the projected output and the electricity price allows it to recover both the generation and transmission investments. In this case, the RE-GenCo would assume all profit risks and uncertainties. However, due to the intermittent nature of the generation output, the RE-GenCo may not want to do so. Instead, the RE-GenCo may seek out a TransCo who is interested in investing in transmission, to bear part of the risks. The risk transfer is consummated by the RE-GenCo paying the TransCo a transmission rate, based on the projected generation performance and electricity prices, for recovering the transmission investment. The payment, measured by a rate λ ($/MWh) multiplied by dispatched renewable energy (MWh), necessitates a negotiation among two parties.

To simplify the discussion, several assumptions are made. First, the utilities are presented in annualized terms in the sense that the calculation is conducted for a typical year with annualized cost components. Second, maintenance costs are not explicitly modeled since an annualized maintenance cost can be included as part of the annual capital investments. Third, a risk neutral attribute is assumed so that the RE-GenCo's utility U_{RG} and the TransCo's utility U_T can be expressed as expected profits of the two participants. These simplifications can be easily relaxed.

3.3.2 Negotiation Process

Two possible outcomes can be reached during a negotiation; an agreement is reached or both parties walk away. For the first outcome, an agreement is reached if the RE-GenCo,

after paying the negotiated transmission rate, can recover its generation investment and, at the same time, the TransCo can recover its transmission investment.

A bilateral contract signed with LSEs is assumed for the RE-GenCo to manage price fluctuations in an electricity market. This assumption is valid since a number of electric utilities have issued long-term (10+ years) power purchase agreements, according to [60]. Considering the projected generation output and a payment to the TransCo, the utility function of the risk-neutral RE-GenCo given a set of future scenarios Ω_S is defined by

$$U_{RG} = E_{s\in\Omega_S} \sum_{t\in\Omega_T} D_t[[FP + SUB - \lambda]P_{Rts} - C_{ts}^{RG}] \tag{14}$$

where $C_{ts}^{RG} = \sum_{b\in\Omega_{I_r}^b} \lambda_{I_r}^b P_{I_r bts}^G$, representing production cost for the RE unit. Note that the generation investment can be included in (14). However, it is, instead, used as the RE-GenCo's threat point, d_{RG}.

If the RE-GenCo does not sign bilateral contracts with LSEs, it confronts an exposure to market price uncertainties. The utility function (14) can be modified to a market-based version U_{RG}^M, taking into account market-based electricity prices at its bus *R* (i.e. Locational Marginal Prices (LMPs)).

$$U_{RG}^M = E_{s\in\Omega_S} \sum_{t\in\Omega_T} D_t[[LMP_{Rts} + SUB - \lambda]P_{Rts} - C_{ts}^{RG}] \tag{15}$$

For the TransCo, if an agreement is achieved, the profit collected by the TransCo from the RE-GenCo's payment with the subtraction of transmission investment can be expressed as

$$U_T = E_{s\in\Omega_S} \sum_{t\in\Omega_T} D_t[\lambda P_{Rts}] - \sum_{k\in\Omega^{CT}} ICT_k Y_k \tag{16}$$

In the alternative in which no agreement is reached, the transmission investment will not occur. In this case, the failure to reach an agreement results in the RE-GenCo utility function arriving at its threat point, d_{RG}, which is set as the stranded RE generation investment, IC_{RG}. Likewise, if the TransCo receives no payment, the TransCo's utility function is settled at its threat point d_T which equals 0.

With knowledge of the utility functions, threat points and projected market conditions, a negotiation process is initiated on the transmission investment plan and the associated transmission rate/payment. The process is depicted in Figure 16. While the two companies negotiate, they anticipate the market operation whose results (LMPs, generation outputs and transmission flows) in turn will affect their attained profit. Therefore, they tend to choose the transmission plan and payment rate which benefit them most.

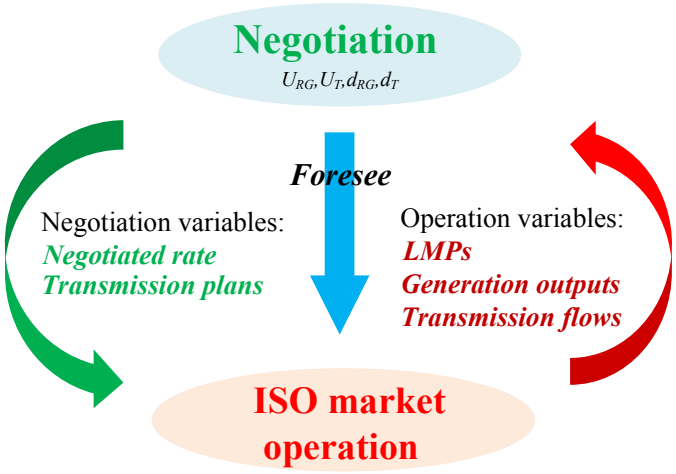

Figure 16. Negotiation between the RE-GenCo and the TransCo

In the negotiation process, both the RE-GenCo and the TransCo take into consideration the intermittent nature of the generation output, the planned transmission capacity with its associated investment cost, and the electricity prices. Due to the complexity

and inter-relationship between the negotiated results and the transmission investment plan, it entails a careful examination of negotiation methodology and solution, which is presented in Section 3.4.

3.3.3 Policy implications on RE subsidies

Optimal transmission investment plans are aimed by policy makers to maximize social surplus, but cannot be directly imposed on merchant transmission investment in a competitive market environment. A possible approach to steer the negotiated transmission investment plans towards the social optimal investment is to make use of the controllable RE subsidy parameter *SUB*, an important component in both companies' utility functions. With everything else unchanged, the negotiated solution can be expressed as a non-linear function of *SUB*. By adjusting this RE subsidy parameter, policy makers then can possibly alter the negotiated solution to match the social optimal transmission investment plan.

The social optimal solution is derived from a centralized transmission planning. The objective is to maximize social surplus (the operation surplus minus transmission investment cost, subject to operation and planning constraints). Contrasting the negotiated solution with the centralized solution, an optimal RE subsidy parameter can be obtained to provide guidance to policy makers. The details of the model construction and comparison are illustrated in Section 3.5.

3.4 Negotiation: A Nash Bargaining Approach

The result between the RE-GenCo and the TransCo in the negotiation process described in Section 3.3 is solved by applying the Nash Bargaining theory. Specifically, a

two-player Nash Bargaining problem and its solution concept are applied to the negotiation problem to derive the analytical model and detailed formulation.

3.4.1 Nash Bargaining

The research on two-person bargaining problems is initiated by Nash [61], [62]. In his seminal work, the bargaining problem is defined when two players, who negotiate over a utility possibility set U, with their threat points $d = (d_1, d_2)$, try to achieve a settlement point $u = (u_1, u_2)$. Nash proved that for every bargaining problem (U, d), there is a unique solution $f(\mathrm{U}, d) = (f_1(\mathrm{U}, d), f_2(\mathrm{U}, d)$ that satisfies the following four axioms.

- Axiom 1. Invariance to linear transformation: For any monotonic linear-affine function H, it requires that $f(H(\mathrm{U}), H(d)) = H(f(\mathrm{U}, d))$. This essentially needs the solution be agnostic of any linear-affine transformations, i.e. shifting and scaling.
- Axiom 2. Symmetry: if $d_1 = d_2$, $(u_1, u_2) \in \mathrm{U}$ and $(u_2, u_1) \in \mathrm{U}$, then $f_1(\mathrm{U}, d) = f_2(\mathrm{U}, d)$. This indicates that the solution should provide equal gains from the cooperation when the feasible utility set U is symmetric.
- Axiom 3. Independence of irrelevant alternatives: for two bargaining problems (U, d) and (U', d), if $f(\mathrm{U}', d) \in \mathrm{U}$, then $f(\mathrm{U}) = f(\mathrm{U}', d)$. It basically says that the addition of irrelevant alternatives does not change the solution.
- Axiom 4. Pareto efficiency: if u and u' are two utility points in a bargaining problem (U, d) and $u' > u$, then $f(\mathrm{U}, d) \neq u$. This axiom requires the pareto-optimality of the bargaining solution.

The unique bargaining solution is then obtained by solving the following optimization problem:

$$f(\mathrm{U}, d) = arg \underset{\substack{(u_1,u_2)>(d_1,d_2) \\ (u_1,u_2)\in \mathrm{U}}}{\text{maximize}} \quad (u_1 - d_1)(u_2 - d_2) \tag{17}$$

The objective is named Nash product, which is later extended in n-person bargaining game [64]. The solution to this problem is referred to as Nash Bargaining Solution (NBS), an important solution concept in game theory, has the properties of simplicity and robustness. Empirical evidences to support NBS are indicated in experimental bargaining theory given in reference [65].

3.4.2 Bargaining on RE Interconnection: An Analytical Model

Suppose that a RE-GenCo has decided to build a RE generating unit at some remote location, and financing of the capital $C_0(\$)$ has been secured. The maximum available output of the RE unit is denoted by $r(MW)$, a random variable with probability density function (pdf) $g(r)$ and cumulative density function (cdf) $G(r)$, subject to the variability of the renewable resource. The model also assumes production cost $C_R(\$/MWh)$ and renewable energy subsidies $S_R(\$/MWh)$ are constant.

As discussed earlier, the RE-GenCo (denoted by subscript *R* in the formulation) seeks out a TransCo (denoted by subscript *T*) to invest in transmission lines to interconnect the RE project and to deliver its output to distance load centers. The per-unit cost to the TransCo for the generation interconnection transmission is represented by $C_T(\$/MWh)$. The price for the renewable energy is represented by a fixed payment $D_R(\$/MWh)$. The two parties negotiate

and try to reach an agreement on the payment rate $\lambda(\$/MWh)$ corresponding to the agreed upon transmission capacity $F_T(MW)$.

Note that the output for the RE generation P_R is constrained by the lower value of the maximum available output r and the transmission capacity F_T, i.e.

$$P_R = min(r, F_T) \tag{18}$$

Using these representations, the RE-GenCo's utility is the expected profit (EP_R),

$$u_R = EP_R \cdot [D_R + S_R - C_R - \lambda] \tag{19}$$

and the TransCo's utility is given as

$$u_T = EP_R \cdot \lambda - F_T C_T \tag{20}$$

Note that their threat points are $(C_0, 0)$.

Applying Nash bargaining theory, the decision variables λ and F_T can be solved by maximizing the Nash Production (*NP*)

$$\max_{\lambda, F_T} NP = [u_R(\lambda, F_T) - C_0] \cdot u_T(\lambda, F_T) \tag{21}$$

The solution can be found if $u_R > 0$ and $u_T > 0$.

Take the first order derivatives with respect to λ and F_T,

$$\frac{\partial NP}{\partial \lambda} = \frac{\partial u_R}{\partial \lambda} u_T + \frac{\partial u_T}{\partial \lambda} [u_R - C_0] \tag{22}$$

$$\frac{\partial NP}{\partial F_T} = \frac{\partial u_R}{\partial F_T} u_T + \frac{\partial u_T}{\partial F_T} [u_R - C_0] \tag{23}$$

Note that EP_R in equations (19) and (20) is a function of F_T due to (18), $EP_R = E_r min(r, F_T)$. When $r>F_T$, $min(r,F_T)=F_T$; when $r<=F_T$, $min(r,F_T)=r$, the expectation then is

$$
\begin{aligned}
EP_R &= F_T \cdot Pr(r > F_T) + Er\,|_{r \le F_T} \\
&= F_T[1 - G(F_T)] + \int_0^{F_T} rg(r)dr \\
&= F_T[1 - G(F_T)] + \int_0^{F_T} d[rG(r)] - \int_0^{F_T} G(r)dr \\
&= F_T - F_T G(F_T) + F_T G(F_T) - \int_0^{F_T} G(r)dr \\
&= F_T - \int_0^{F_T} G(r)dr
\end{aligned}
\tag{24}
$$

From (24), the partial derivative of EP_R with respect to F_T can be expressed as

$$\frac{\partial EP_R}{\partial F_T} = 1 - G(F_T) \tag{25}$$

The partial derivative of u_R and u_T with respect to λ and F_T can be obtained, i.e.,

$$\partial u_R / \partial \lambda = -EP_R \tag{26}$$

$$\partial u_R / \partial F_T = [1 - G(F_T)] \times [D_R + S_R - C_R - \lambda] \tag{27}$$

$$\partial u_T / \partial \lambda = EP_R \tag{28}$$

$$\partial u_T / \partial F_T = [1 - G(F_T)] \times \lambda - C_T \tag{29}$$

Insert equations (26)-(29) into equations (22) and (23),

$$\frac{\partial NP}{\partial \lambda} = -EP_r \times u_T + EP_R[u_R - C_0] \tag{30}$$

$$\frac{\partial NP}{\partial F_T} = [1 - G(F_T)][D_R + S_R - C_R - \lambda] \times u_T + [[1 - G(F_T)]\lambda - C_T][u_R - C_0] \tag{31}$$

The solution can be found when the above two equations equal to 0. Then equation (30) becomes

$$EP_R[u_R - C_0 - u_T] = 0 \tag{32}$$

The expected RE output EP_R is normally positive, and hence (32) satisfies only when

$$u_R - C_0 = u_T \tag{33}$$

which is the logical outcome in which the utility is equally divided between the RE-GenCo and the TransCo.

The relation between λ and F_T can be derived by replacing u_R and u_T in (33) with (19) and (20)

$$EP_R[D_R + S_R - C_R - \lambda] - C_0 = EP_R\lambda - F_T C_T \tag{34}$$

Re-expressing the equation, one obtains

$$\lambda = \frac{D_R + S_R - C_R}{2} - \frac{C_0 - F_T C_T}{2EP_R} \tag{35}$$

Similarly, set equation (31) equal to 0, replace $u_R - C_0$ with u_T, and omit positive u_T. Equation (31) can be rewritten as

$$[1 - G(F_T)][D_R + S_R - C_R] - C_T = 0 \tag{36}$$

F_T then can be solved in the following explicit form

$$F_T = 1 - G^{-1}\left(\frac{C_T}{D_R + S_R - C_R}\right) \tag{37}$$

and λ can be found by replacing F_T in (35) with (37).

It is observed the negotiated payment rate λ and invested transmission capacity F_T can be explicitly determined in this model with the consideration of the RE output uncertainty. However, since the transmission investment is lumpy in nature, the transmission plan is likely to consist of a set of discrete transmission candidates. Hence a more careful examination of the negotiation process and a detailed formulation to handle the lumpy investment are needed.

3.4.3 Bargaining on RE Interconnection: A Detailed Formulation

The bargaining process on RE interconnection is formulated as a bi-level optimization problem. The Nash product is maximized in the upper level problem, while a set

of lower problems represents the market operations anticipated by the RE-GenCo and the TransCo, for every hour *t* and scenario *s*.

The detailed formulation is given below, with the RE-GenCo's utility U_{RG} and the TransCo's utility U_T denoted by (14) and (16). Suppose the negotiation is intended to connect the RE unit I_r at Bus *r*, the bargaining problem is then formulated as:

$$\max_{\lambda, Y_k} \left[U_{RG}(P_{Rts}, \lambda) - IC_{RG}\right] \times U_T(\lambda, P_{Rts}, Y_k) \tag{38}$$

Subject to

$$U_{RG}(P_{Rts}, \lambda) \geq IC_{RG} \tag{39}$$

$$U_T(\lambda, P_{Rts}, Y_k) \geq 0 \tag{40}$$

$$-M \sum_{k \in \Omega^{CT}} Y_k \leq \lambda_R \leq M \sum_{k \in \Omega^{CT}} Y_k \tag{41}$$

$$P_{Rts} = \sum_{b \in \Omega^b_{I_r}} P^G_{I_r bts} \tag{42}$$

where $P_{Rts}, \forall t \in \Omega_T, \forall s \in \Omega_S =$

$$\underset{P^G_{ibts} P^L_{jbts}}{arg\max} \quad \sum_{j \in \Omega^L_n} \sum_{b \in \Omega^b_j} \lambda^L_{jb} P^L_{jbts} - \sum_{i \in \Omega^G} \sum_{b \in \Omega^b_i} \lambda^G_{ib} P^G_{ibts} \tag{43}$$

Subject to

$$\sum_{j \in \Omega^L_n} \sum_{b \in \Omega^b_j} P^L_{jbts} + \sum_{k|o(k)=n} F_{kts} - \sum_{k|r(k)=n} F_{kts} = 0, \quad (LMP_{nts}), \forall n \in \Omega_N \tag{44}$$

$$0 \leq P^G_{ibts} \leq \bar{P}^G_{ib}, \forall i \in \Omega^{TG}, \forall b \in \Omega^b_i \tag{45}$$

$$0 \leq P^G_{ibts} \leq \bar{P}^G_{ibts}, \forall i \in \Omega^{RG}, \forall b \in \Omega^b_i \tag{46}$$

$$F_{kts} = \frac{1}{X_k}[\delta_{o(k)ts} - \delta_{r(k)ts}], \forall k \in \Omega^{ET} \tag{47}$$

$$-\bar{F}_k \leq F_{kts} \leq \bar{F}_k, \forall k \in \Omega^{ET} \tag{48}$$

$$-(1-Y_k)M \leq F_{kts} - \frac{1}{X_k}[\delta_{o(k)ts} - \delta_{r(k)ts}] \leq (1-Y_k)M, \forall k \in \Omega^{CT} \tag{49}$$

$$-Y_k \bar{F}_k \leq F_{kts} \leq Y_k \bar{F}_k, \forall k \in \Omega^{CT} \tag{50}$$

The upper level problem, consisting of equations (38)-(40), reflects the requirement in Nash bargaining problem. Inequality (41) is an additional constraint demanding zero payment if no transmission line is invested. Equality (42) collects the total dispatched renewable energy output from all offer blocks of the RE unit which is to be interconnected. For each hour *t* and scenario *s*, a corresponding lower-level problem (43)-(50) reflects the market operation with LMPs, dispatched generation output, and transmission flow. The objective of the lower-level problems (43) is to maximize market operation net surplus. Constraint (44) enforces real power balance at each bus. Constraints (45) and (46) impose generation capacity limit on non-renewable and renewable generating units, respectively. Note that the maximum available output for some RE unit *i*, $\overline{P}^{G}_{ibts}$ varies in hours and scenarios, allowing for the variability of renewable resources.

Constraints (47)-(50) enforce transmission limits for existing and candidate transmission lines. Regarding constraint (49), the constraint is active and *M* is set at 0 when Y_k = 1 or the investment decision is affirmative. However, if Y_k = 0 or the investment decision is negative, *M* is set to be a large number meaning that this constraint is not active and therefore not considered.

This formulation could be modified to consider market-based renewable energy price (LMPs) received by the RE-GenCo, if it does not enter into a bilateral contract. Its utility function in objective function (38) can be replaced by $U^{M}_{RG}(LMP_{Rts}, P_{Rts}, \lambda)$ given in equation (15). The utility function is now determined by both the renewable energy production P_{Rts} and its market price LMP_{Rts}.

3.5 Implications on Renewable Subsidy Policy

A centralized transmission planning model is described in this section that will provide a benchmark of social optimal transmission investment, for contrasting the negotiated transmission plans described in Section 3.4. Policy implications on renewable energy subsidies will be derived by proposing an analytical model and a detailed formulation, where renewable subsidies are used as a critical and adjustable parameter to steer the negotiated solution towards a centralized solution.

3.5.1 Centralized Planning and Policy Implication

Suppose a centralized planner, who performs the traditional Integrated Resource Planning function, decides to interconnect a RE unit by planning and investing in a new transmission line. Considering the benefit B_R ($/MWh) from the renewable energy, the centralized planner needs to make a decision on the invested transmission capacity F_T to maximize social surplus:

$$\underset{F_T}{\text{maximize}} \quad SS = EP_R \times B_R - EP_R \times C_R - F_T C_T \tag{51}$$

The same notation in Section 3.4.2 is used in (51). Take the derivative of SS with respect to F_T and set it equal 0, i.e.,

$$\frac{dSS}{dF_T} = \frac{dEP_R}{dF_T}[B_R - C_R] - C_T \tag{52}$$

$$0 = [1 - G(F_T)][B_R - C_R] - C_T \tag{53}$$

F_T in the centralized planning model can be solved explicitly as follows,

$$F_T = 1 - G^{-1}\left(\frac{C_T}{B_R - C_R}\right) \tag{54}$$

Comparing the negotiated solution (37) with the centralized solution (54), the adjustable parameter of renewable energy subsidies, S_R can be utilized to steer the negotiated solution towards the benchmark solution by equating (37) and (54),

$$D_R + S_R - C_R = B_R - C_R \tag{55}$$

$$S_R = B_R - D_R \tag{56}$$

Equation (56) indicates that the optimal renewable energy subsidies should be set as the difference between the benefit from the RE generation and the payment for purchasing renewable energy. Of course, determining the benefit received is not a trivial task. In any event, policy makers can use this result as guidance for renewable energy subsidy policy, and establish a subsidy mechanism that provides merchant investors with sufficient market incentives for achieving social optimal transmission investment plans.

3.5.2 An Illustrative Example

A simple example is presented to illustrate the principle of the negotiation model and demonstrate the important role of policy in moving the bargaining solution to an idealistic solution that is societal beneficial.

The bi-level negotiation process depicted in Section 3.4 is elaborated by means of the payoff matrix. The solutions for the negotiation model, in the two situations with or without renewable energy, are compared with that in the centralized model.

As shown in Figure 17, a RE-GenCo is going to make a decision on a wind farm investment. The company has two options.

- Option [1]: Investing at location [1] with cost \$2/MW, it will be able to generate 19MWh wind energy at the price of \$1/MWh, and pay a rate λ_{R1} to the TransCo for transmission investment cost recovery.
- Option [2]: Investing at location [2] with cost \$2/MW, it will be able to generate 13MWh wind energy at the price of \$1/MWh, and pay a rate λ_{R2} to the TransCo for transmission investment cost recovery.

Similarly, the TransCo has two options as follows:

- Option (1): TransCo will build the transmission along path (1) with capacity 19MW; its investment cost is \$10, and TransCo receives λ_{R1} from the GenCo.
- Option (2): TransCo will build the transmission along path (2) with capacity 13MW; its investment cost is \$4, and TransCo receives λ_{R2} from the GenCo.

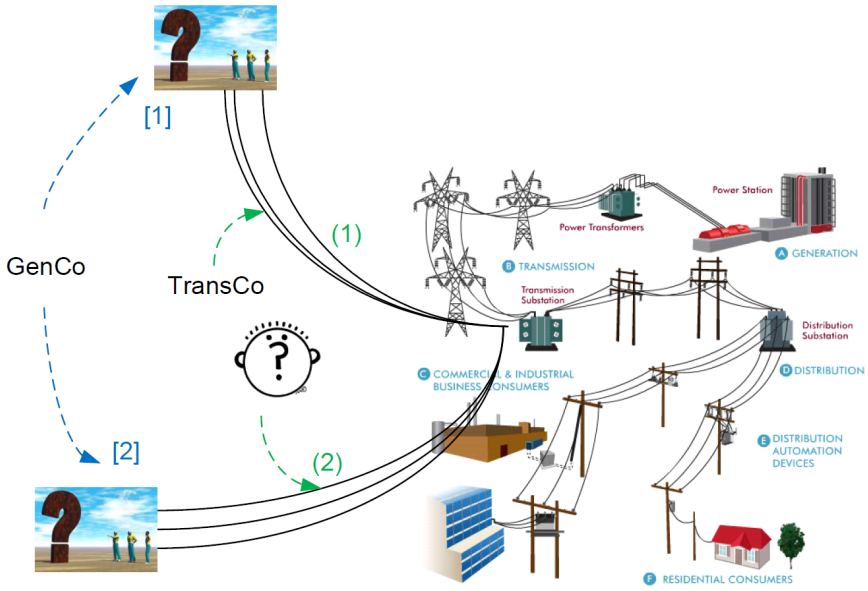

Figure 17. Options for renewable generation and transmission investment

Correspondingly, LSE will receive three different levels of benefit, depending on the negotiation results of the RE-GenCo and the TransCo.

- Benefit (a): If both the GenCo and the TransCo choose [1] and (1), LSE will have a utility level of $14.
- Benefit (b): If they choose [2] and (2), LSE will have a utility level of $10.
- Benefit (c): LSE will have 0 otherwise.

In the first case there is no renewable energy subsidy, the payoff matrix for the GenCo and the TransCo then can be expressed as follows:

		TransCo (1)	TransCo (2)
GenCo	[1]	$(19\times1-2-\lambda_{R1}, \lambda_{R1}-10)$	(-2,-4)
	[2]	(-1,-6)	$(13\times1-1-\lambda_{R2}, \lambda_{R2}-4)$

Their negotiated result is the solution to maximize the product of their utilities, for example, $\max_{\lambda_{R1}} [19\times1-2-\lambda_{R1}][\lambda_{R1}-10]$. Therefore, the solutions are $\lambda_{R1}=13.5$, $\lambda_{R2}=8$.

The payoff matrix is then

		TransCo (1)	TransCo (2)
GenCo	[1]	(3.5,3.5)	(-2,-4)
	[2]	(-1,-6)	(4,4)

The payoff matrix for LSE is determined by the negotiated result of the GenCo and the TransCo.

		TransCo (1)	TransCo (2)
GenCo	[1]	14	0
	[2]	0	10

Following the analysis of Nash Bargaining theory, the GenCo and the TransCo will choose the option ([2], (2)) which maximizes their utility levels since Nash Product of (4, 4) is greater than (3.5, 3.5).

Nevertheless, considering the social surplus which now involves the utility level from LSE besides the two negotiators, the social optimal investment plan should be settled at ([1], (1)). Indeed, the total social surplus achieved by ([1], (1)), 3.5+3.5+14=21, clearly exceeds the total social surplus by ([2], (2)), 4+4+10=18.

In this case, the negotiated result does not match the centralized investment plan. Hence, the social surplus maximization is not achieved.

Now consider how subsidy can help to steer the negotiated result to a centralized social optimal solution. Suppose the RE-GenCo is subsidized by \$0.5/MWh. The revenue stream of the RE-GenCo now includes this subsidy in addition to the original energy sale. Note that this subsidy will not alter the optimal solution for the centralized model; rather, it will only re-distribute the total social surplus.

However, the payoff matrix for the RE-GenCo and the TransCo has been changed:

		TransCo (1)	TransCo (2)
GenCo	[1]	$(19\times1-2-\lambda_{R1}+19\times0.5, \lambda_{R1}-10)$	(-2,-4)
	[2]	(-1,-6)	$(13\times1-1-\lambda_{R2}+13\times0.5, \lambda_{R2}-4)$

The two companies negotiate the payment rate under the different investment plans, resulting in $\lambda_{R1}=18.25$ or $\lambda_{R2}=11.25$.

The numerical representation of the matrix becomes

		TransCo (1)	TransCo (2)
GenCo	[1]	(8.25,8.25)	(-2,-4)
	[2]	(-1,-6)	(7.25,7.25)

Apparently, Option ([1], (1)) outperforms Option ([2], (2)) in terms of greater utility levels for both companies. Therefore, ([1], (1)) becomes the new negotiated result in this subsidy environment. The subsidy \$0.5/MWh indeed plays a crucial role in steering the negotiated solution to a centralized solution and successfully achieves social optimality.

3.5.3 Centralized Planning: A Detailed Formulation

The detailed formulation of the centralized planning model, which allows for uncertainties and realistic constraints, is presented below.

$$\underset{P^G_{ibts},P^L_{jbts},Y_k}{\text{maximize}} E_{s\in\Omega_S}\sum_{t\in\Omega_T} D_t[\sum_{j\in\Omega^L}\sum_{b\in\Omega^b_j}\lambda^L_{jb}P^L_{jbts}-\sum_{i\in\Omega_G}\sum_{b\in\Omega^b_i}\lambda^G_{ib}P^G_{ibts}]-\sum_{k\in\Omega^{CT}} ICT_k Y_k \qquad (57)$$

Subject to

$$\forall t\in\Omega_T, \forall s\in\Omega_S$$

(44)— (50)

The objective function is to maximize social surplus composed of operation surplus minus the transmission investment cost. The operation constraints are identical with the ones in the negotiated model as given in equations (44)-(50).

3.6 Numerical Results

3.6.1 Garver's Six-Bus Test Case

The detailed formulation for the negotiation on RE interconnection is studied with Garver's six-bus test case in Figure 18, which comprises six buses, six existing transmission lines, three generating units, and five loads. The generator at Bus 6 is assumed to be a RE or wind resource. In this study, transmission lines between Bus 6 and the grid are needed to deliver the RE output to the load. The supply offer and demand bid data for the two traditional generators and 5 loads are given in Table 9. The number and size of blocks vary for each market participant.

A constant production cost is assumed for the wind generator WG3 at Bus 6 and its cost and operation data are given in Table 10. The third column is its investment cost IC_{RG} that will be used as the RE-GenCo's threat point in the negotiation process. The renewable energy contract price FP is given in the fourth column. P_{rate} denotes the nameplate capacity of the wind unit. The maximum possible output P_{max} is characterized by the non-linear function between wind speed v and P_{rate} with three parameters of WG3: cut-in, cut-out and rated wind speed V_{ci}, V_{co} and V_{rate}. The non-linear feature can be described by the following [30]:

$$P_{max} = \begin{cases} 0 & 0 \le v < v_{ci} \\ P_{rate}(v - V_{ci}) / (V_{rate} - V_{ci}) & V_{ci} \le v < V_{rate} \\ P_{rate} & V_{rate} \le v \le V_{co} \\ 0 & V_c o < v \end{cases} \tag{58}$$

Table 9. Generator and load data

Generators				Loads		
Bus	G	Offer Size (MW)	Offer Price ($/MWh)	L	Bid Size (MW)	Bid Price ($/MWh)
1	G1	[200;100;100]	[21;23;28]	L1	[40;40]	[43;30]
2				L2	[80;80;80]	[54;50;48]
3	G2	[210;210;140]	[30;34;43]	L3	[20;20]	[30;26]
4				L4	[80;80]	[45;32]
5				L5	[80;80;80]	[50;42;30]

Table 10. Wind unit data

Bus	Name	Investment Cost ($10^6$$)	Cost ($/MWh)	*FP*	P_{rate}	V_{ci}	V_{rate}	V_{co}
6	WG3	10	2	12	600	4	10	22

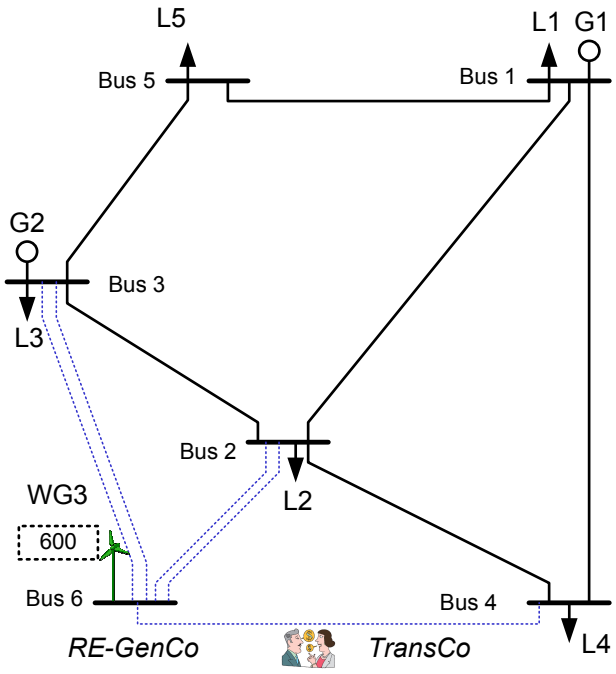

Figure 18. Garver's six-bus test system

Table 11. Transmission data

Name	From Bus	To Bus	Reactance (Ω)	Limit (MW)	Cost (10^6\$)	Type
T1	1	2	0.4	250	-	E(xisting)
T2	1	4	0.6	220	-	E
T3	1	5	0.2	300	-	E
T4	2	3	0.2	300	-	E
T5	3	5	0.2	300	-	E
T6	2	6	0.3	150	8.0	C(andidate)
T7	2	6	0.15	300	13	C
T8	3	6	0.4	150	9.2	C
T9	3	6	0.3	200	10	C
T10	4	6	0.3	200	11	C

Table 11 presents the data for the existing and candidate transmission lines. Five transmission investment candidates (T6-T10) are proposed with the intent to connect Bus 6 to the grid. The pattern of transmission costs follows the economies of scale, e.g. building one 300-MW line between Buses 2 and 6 is less expensive than building two 150MW lines connecting these two buses.

To accommodate the variability from wind resource, three scenarios of wind speed are constructed for four subperiods in a year, which are represented by four seasons with equal time duration, i.e. $\frac{1}{4}8760h = 2190h$. The wind speed data in each scenario and subperiod is given in

Table **12**. Using the function (58), the maximum possible output of WG3 can be calculated, and the result is shown in Table 13. Note that the wind unit normally generates more renewable energy during the Fall and Winter season due to ample wind resources.

Table 12. Scenarios of wind speed in four subperiods

Scenario	Spring	Summer	Fall	Winter
S1=High wind	7	5	10	9
S2=Medium wind	5	5	8	9
S3=Low wind	2	1	5	8

Table 13. Maximum possible output of wind energy

Scenario	Spring	Summer	Fall	Winter
S1=High wind	300	100	600	500
S2=Medium wind	100	100	400	500
S3=Low wind	0	0	100	400

3.6.2 The Negotiated Solution with Renewable Energy Contract Price *FP*

All combinations of the 5 transmission candidates were examined and no negotiation solution is reached without a subsidy. The renewable energy subsidy is then fixed at *SUB*=$5/MWh and the negotiated solutions are examined using renewable energy contract price *FP*. The negotiated transmission investment plan Y_N is reported in Table 14. The negotiated payment λ and the attained utility levels for each party are given in Table 15.

Table 14. Negotiated transmission investment decision Y_N

Candidate	Y_6	Y_7	Y_8	Y_9	Y_{10}
Decision	0	1	0	0	0

Table 15. Negotiated results of payment rate and attained utilities

$U_{RG}(10^6\$)$	U_{RG}-$IC_{RG}(10^6\$)$	$U_T(10^6\$)$	λ_R (\$/MWh)
10.54	0.54	0.54	8.43

It is observed that in the settlement, the RE-GenCo would like to pay the TransCo \$8.43/MWh for recovering the cost of transmission investment on candidate line 7. The value of the 2nd and 3rd columns are identical, indicating the utility function for the RE-GenCo is the same as the utility function for the TransCo (i.e. equal utility split) which verifies equation (33) established in the analytical model for bargaining over transmission investment.

3.6.3 The Negotiated Solution with Market-Based Price *LMP*

Although most renewable energy developers enter into bilateral contracts to secure a fixed electricity price, they can also choose to receive LMPs in market settlement. In this situation, its market-based utility function U_{RG}^M is used in the negotiation process. Using the same subsidy parameter *SUB* at \$5/MWh, the new investment transmission plan Y_N^M and the associated utility levels are shown in Table 16.

The market-based negotiation results show more transmission investments. Specifically, the resulted plan suggests building 2 lines to Bus 2 and 1 line to bus 3, making the wind generator bus an integral part of the system. Comparing Table 16 with Table 15, a significantly higher utility and transmission rate are also attained. For example, U_T is raised from \$0.54 million to \$11.73 million and the negotiated rate is \$18.88/MWh .The increases

are due primarily to higher generator revenues from LMPs than that obtained from contract price *FP*.

Table 16. Negotiated transmission plan Y_N^M and utility levels

Trans plan	Y_6	Y_7	Y_8	Y_9	Y_{10}
	1	1	0	1	0
Utility levels	U_{RG}^M	U_{RG}^M -IC_{RG}	U_T	λ_R	
	21.73	11.73	11.73	18.88	

By investing in the 3 lines and transforming the generator bus into a system bus, the RE generator output are not constrained in any scenarios. Hence, the energy price or LMP for the RE generator output is always determined by the system marginal units and not by the cheaper wind generator. As a result, the expected higher generator revenue due to higher market-based price (LMP) allows the RE-GenCo to make higher profits and to pay for additional transmission.

3.6.4 Centralized Transmission Planning

In Section 3.5.1, an optimal RE subsidy parameter *SUB* is explicitly obtained for steering the negotiated solution on transmission investment to the social optimal solution. This section will examine the possibility of adjusting RE subsidy parameter to achieve the goal in a more comprehensive formulation.

As shown in Section 3.5.3, optimization problem (57) is solved for the centralized solution targeting to maximize social surplus. The solution Y_C is then obtained in Table 17.

Table 17. Centralized transmission investment decision Y_c

Candidate	Y_6	Y_7	Y_8	Y_9	Y_{10}
Decision	1	1	0	0	0

Compared to previous negotiated results, candidate line T6 and T7 are the 2 lines to be invested by the centralized planning in order to maximize the social surplus. The achieved social surpluses under different investment decisions are compared in Table 18. The centralized planning gives the maximum social surplus, while the negotiated decision, when the RE-GenCo is settled at market-based prices—LMPs, results in the lowest social surplus. This is not surprising since the negotiation between the RE-GenCo and the TransCo is focused on their profits from the investment decision and not on the overall social surplus. Y_N gives low social surplus due to underinvestment in transmission lines (T7), and Y_N^M results in an even lower social surplus due to the overinvestment in transmission lines (T6, T7 and T9).

Table 18. Social surplus under different investment decisions

Decisions	Y_N	Y_N^M	Y_C
Social Surplus ($\$10^6$)	137.96	136.38	142.55

3.6.5 RE Subsidy Sensitivity Analysis

This section is concerned with the possibility of adjusting the subsidies *SUB* to drive the negotiated solution towards the maximum social surplus derived from the centralized planning decision. The sensitivity analysis of *SUB* on transmission planning decisions and negotiated payment rate are shown in Figure 19-Figure 21.

Note that the simulation result includes the use of negative values for *SUB*, representing penalties rather than subsides for generating renewable energy. This negative

value can be used to model cost overrun, high financial charges on capital, or costs incurred from project delay.

Figure 19 shows that there is no negotiated transmission plan when *SUB* is between \$-10/MWh and \$5/MWh. When *SUB* is between \$7/MWh and \$41/MWh, the negotiated result is [1 1 0 0 0], which is exactly the centralized plan and the maximum social surplus solution. Beyond \$42/MWh, even though the higher subsidies would afford more transmission investments, the resultant social surplus is less than the case when the subsidy is between \$7/MWh to \$41/MWh. This implies that, policy makers can always increase subsidies to incentivize transmission investments to attain the maximum social surplus goal. Nevertheless, excessive subsidies can lead to more transmission but not necessarily higher overall social surplus.

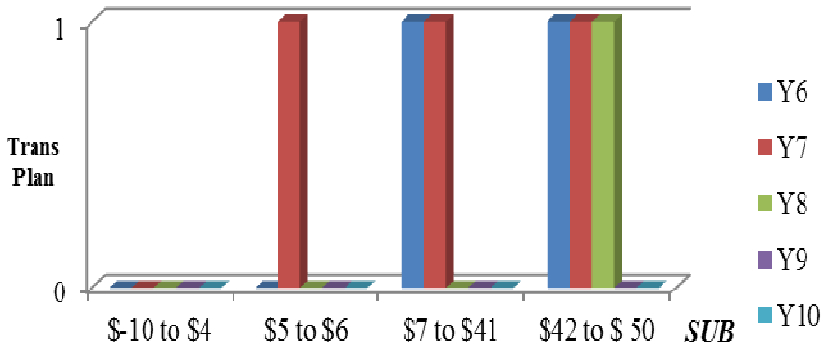

Figure 19. Transmission plan variation under *SUB* with contract price *FP*

However, when RE-GenCo receives *LMP* instead of *FP*, Figure 20 shows that the subsidy *SUB* has limitations to function as a controllable parameter for steering the negotiated transmission investment decision to the social optimal solution. This implies that,

due to the LMP uncertainty, subsidies may help to reach an investment decision but may be restricted for achieving social optimal investment plans.

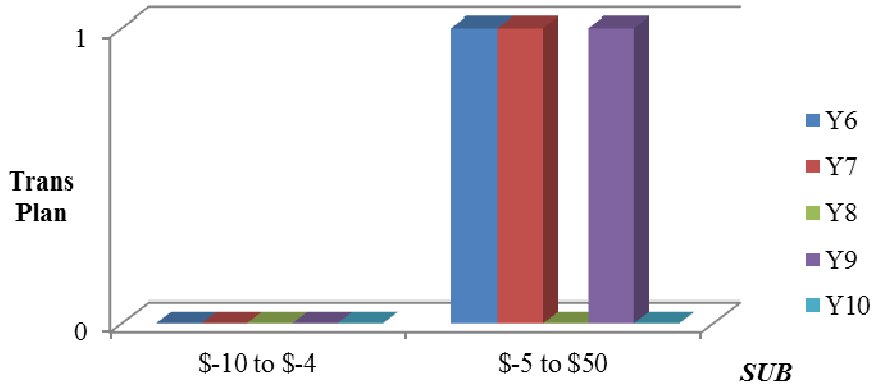

Figure 20. Transmission plan variation under *SUB* with market-based price *LMP*

This observation is further demonstrated in Figure 21 and Figure 22 in which the negotiated transmission rate increases piece-wise linearly with subsidies. Figure 21 also shows step changing of λ_R when *SUB* alters the negotiated transmission plans. However, Figure 22 exhibits only one-time step up of payment rate when subsidies are sufficient to form an agreement in the negotiation. No more step changing but only linear changing of λ_R is shown after the agreement, due to the limited controllability of subsidies.

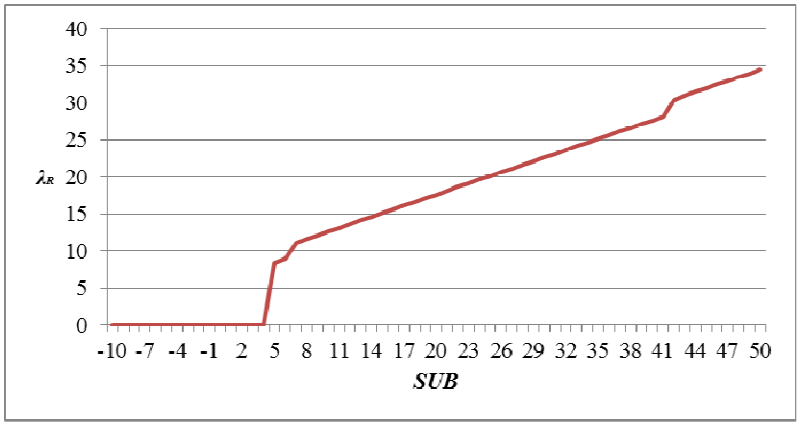

Figure 21. Payment rate variation under *SUB* with contract price *FP*

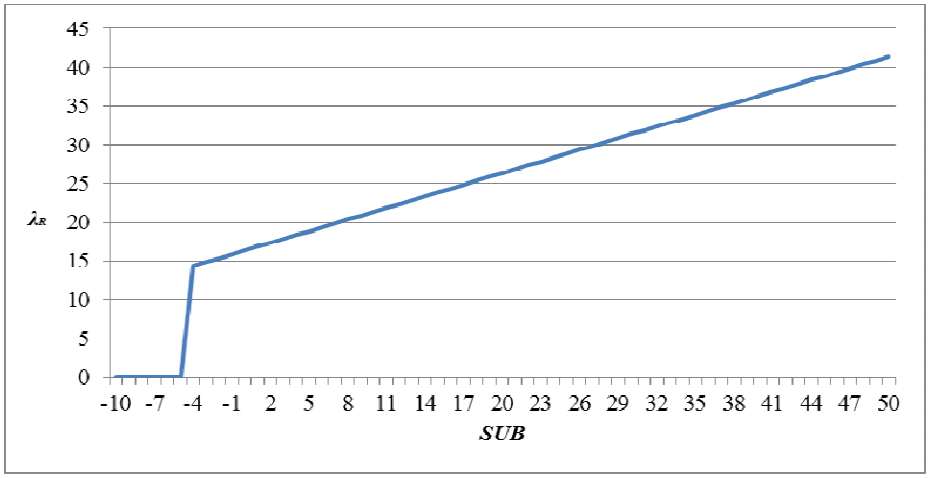

Figure 22 Payment rate variation under *SUB* with market-based price *LMP*

Based on the observations, this case study leads to the following suggestions:

(1) The Nash Bargaining theory guides the negotiation process. The results show that the RE-GenCo and the TransCo equally split utilities attained from renewable energy investment. The Nash Bargaining solution renders a fair and efficient utility allocation between the two companies.

(2) Subsidies are critical for RE-GenCos and TransCos to reach an investment agreement during the proposed negotiation process. It can also steer the negotiated solution to the centralized solution which achieves maximum social surplus when the electricity price is fixed through renewable energy contracts.

(3) Due to market price uncertainties, the controllability of subsidies is limited when RE-GenCos do not sign a renewable energy contract. This limitation needs to be recognized in the design of subsidies.

CHAPTER 4. CONCLUSION

4.1 Summary of the Dissertation

This dissertation addresses the issues associated with the short-term transmission operation and long-term transmission planning. A congestion forecasting algorithm is developed to assist market operators and market participants in short-run decision making. In long-term transmission planning, the issues of negotiation and policy making for integrating renewable energy are investigated.

Short-term congestion forecasting is critical for both market traders and market operators. Congestion forecasting helps to explain electricity price behaviors and facilitates decision making of power market participants.

In Chapter 2, this dissertation proposes a basic scenario-conditioned forecasting algorithm that permits the short-term forecasting of congestion, prices, and other power system variables conditional on a given generating unit commitment pattern and transmission network topology. This basic algorithm uses the novel concept of "system pattern" to permit structural capacity constraints on generation and transmission to be taken into consideration in the forecasting procedure.

To handle practical data-availability concerns, an extension of this basic algorithm is then proposed in a probabilistic framework that can be implemented on the basis of publicly available information. The accuracy of this probabilistic algorithm relative to a more traditional GARCH statistical forecasting model is demonstrated with a NYISO case study.

A cross-scenario extension of this forecasting algorithm is proposed in which probabilities are assigned to different scenarios. This permits forecasters to probabilistically

average forecasts across distinct scenarios, allowing the use of longer forecast horizons and/or increasingly available historical data.

Chapter 3 is concerned with the issue of transmission investment to integrate renewable energy. A negotiation methodology has been proposed between a renewable energy developer and a transmission company for sharing renewable energy uncertainties and market risks.

The rate or payment, which is paid by the RE developer to the TransCo for transmission cost recovery, is established via a negotiation methodology based on Nash Bargaining theory. Both the analytical and numerical solutions of the transmission plan and payment are derived for the negotiation. The practicality of the proposed approach and the Nash Bargaining solution provide important investment guidance to both generation and transmission developers.

If the projected generation performance and market prices do not render an agreement, a renewable energy subsidy may be needed to incentivize transmission projects to meet the RPS requirement. The proposed approach can be used by policy makers to develop a proper subsidy to RE developer for reaching an agreement in a negotiation.

The findings show that transmission investment plans and payment rate can be effectively determined in the negotiation using the Nash bargaining approach. By comparing the negotiation and the centralized planning model, an optimal subsidy policy can be obtained to achieve maximum social surplus. It is also recognized that the controllability of subsidies is limited due to electricity price uncertainties when RE-GenCos sign no renewable energy contracts.

4.2 Future Work

The two approaches for transmission operation and planning are developed under some assumptions. The future work can be aimed at more generalized and practical approaches with realistic considerations.

In Chapter 2, the proposed algorithm is targeted for energy-only markets; future work should consider the incorporation of ancillary services. Future work can also explore additional factors, such as possible strategic supply offer behaviors by generators. Moreover, alternative forms for the probabilistic point inclusion test, a key building block of the proposed algorithm, will be systematically studied.

In Chapter 3, future work can consider the use of more realistic scenarios for handling renewable energy uncertainties by exploiting more advanced scenario generation methods, for example, a moment-matching method developed in [66]. Future work could also be the extension of this approach to a multi-player negotiation that consists of multiple market participants including LSEs, policy makers, additional RE and transmission developers. Furthermore, the issue of asymmetric accessible information for different market participants should be examined.

APPENDIX. PROOF

Consider a wholesale power market operating over a transmission grid with N buses. Assume for simplicity that each bus i has one fixed load denoted by L_i and one generator with a real power level denoted by P_i. Suppose, also, that each generator i has a quadratic total cost function with coefficients a_i and b_i. Finally, suppose the objective of the market operator in each hour is to minimize the total system cost of meeting fixed load subject to an injection-equals-load balance constraint, transmission line flow limits, and generator operating capacity limits.

In particular, suppose the market operator attempts to achieve its objective in each hour by using the following standard DC-OPF formulation that assumes a lossless transmission system:

$$\min_{P} \sum_{i=1}^{N} [a_i P_i + b_i P_i^2] \tag{59}$$

$$s.t. \ \sum_{i=1}^{N} P_i - \sum_{i=1}^{N} L_i = 0 : \ \lambda \tag{60}$$

$$\sum_{i=1}^{N} \beta_{ij} [P_i - L_i] \le \mathrm{F}_\mathrm{j}^{+} : \ \mu_j^{+}, \ \text{for } j = 1:T \tag{61}$$

$$-\sum_{i=1}^{N} \beta_{ij} [P_i - L_i] \le \mathrm{F}_\mathrm{j}^{-} : \ \mu_j^{-}, \ \text{for } j = 1:T \tag{62}$$

$$P_i \le Cap_i^U : \ \sigma_i^U, \ \text{for } i = 1:N \tag{63}$$

$$-P_i \le -Cap_i^L : \ \sigma_i^L, \ \text{for } i = 1:N \tag{64}$$

In these equations, β_{ij} denotes the *Generation Shift Factor (GSF)* that measures the impact of 1MW injection by generator i on transmission line j. Equality (60) represents the system balance constraint ensuring total generation matches total load. The transmission line

flow limit constraints in two directions are expressed in (61) and (62). The last two inequalities (63) and (64) express each generator's upper and lower operating capacity limits.

Proposition 1: *Consider the standard DC-OPF formulation with fixed loads and quadratic generator cost functions described in (59) through (64). Suppose this standard formulation is used by a market operator to determine system variable solutions. Then, conditional on any given commitment-and-line scenario S, the load space can be covered by convex polytopes such that: (i) the interior of each convex polytope corresponds to a unique system pattern; and (ii) within the interior of each convex polytope the system variable solutions can be expressed as linear-affine functions of the vector of distributed loads.*

Proof Outline [44]: First note that the DC-OPF formulation can equivalently be expressed in the following compact form:

$$\min_{P} \frac{1}{2} P^T H P + \alpha^T P \tag{65}$$

$$s.t. \quad G_1 P = W_1 + S_1 L : \quad \Lambda_1 \tag{66}$$

$$\text{and, for} \quad i = 2 : (1 + 2N + 2T)$$

$$G_i P \le W_i + S_i L : \quad \Lambda_i \tag{67}$$

The notation in this general QP problem is described in [44]. The *KKT* first-order necessary conditions for (65)-(67) can then be expressed as follows:

$$HP + \alpha + G^T \Lambda = 0 \tag{68}$$

$$G_1 P - W_1 - S_1 L = 0 \tag{69}$$

$$\text{and, for } i = 2 : (1 + 2N + 2T),$$

$$\Lambda_i (G_i P - W_i - S_i L) = 0 \tag{70}$$

$$\Lambda_i \ge 0 \tag{71}$$

$$G_i P - W_i - S_i L \le 0 \tag{72}$$

Let A denote the set of indices corresponding to the active (binding) equality and inequality constraints for the DC-OPF problem. If the number of binding unit capacity constraints and line limit constraints are denoted by R and M, respectively, then Cardinality(A) = $1+R+M$. Let G^{A}, W^{A} and S^{A} represent the matrices corresponding to A. Then, G^{A}, W^{A} and S^{A} have row dimension $1+R+M$ and column dimension N. Let Λ^{A} denote the multiplier vector corresponding to A. Given A, equations (68)-(70)reduce to

$$G^{\mathrm{A}} P - W^{\mathrm{A}} - S^{\mathrm{A}} L = 0 \tag{73}$$

$$HP + \alpha + (G^{\mathrm{A}})^T \Lambda^{\mathrm{A}} = 0 \tag{74}$$

Tøndel [46] defines the *linear independence constraint qualification (LICQ)* for an active set of constraints to be the assumption that these constraints are linearly independent. For the problem at hand, LICQ holds if G^{A} has full row rank. A generator that is at its upper capacity limit cannot at the same time be at its lower limit, hence [1 0 · · · 0] and [−1 0 · · · 0] never co-exist. Moreover, the GSF matrix included in G^{A} has linearly independent rows. Thus, rank(G^A) = min[$1+R+M$, N]. It follows that G^{A} has full row rank $1+R+M$ if

$$1 + R + M \le N \tag{75}$$

The regularity condition (75) requires that the number of binding constraints [$1+R+M$] does not exceed the number of decision variables N, a necessary condition for the existence of the DC-OPF problem solutions assumed to exist in Proposition 1. Consequently, (75) automatically holds under the assumptions of Proposition 1.

$$\Lambda^{\mathrm{A}} = -\left[G^{\mathrm{A}} H^{-1} (G^{\mathrm{A}})^T\right]^{-1} \left[G^{\mathrm{A}} H^{-1} \alpha + W^{\mathrm{A}} + S^{\mathrm{A}} L\right] \tag{76}$$

$$P = -H^{-1}\alpha + H^{-1}(G^{\mathrm{A}})^T \left[G^{\mathrm{A}} H^{-1} (G^{\mathrm{A}})^T\right]^{-1} \left[G^{\mathrm{A}} H^{-1} \alpha + W^{\mathrm{A}} + S^{\mathrm{A}} L\right] \tag{77}$$

$$0 \le \left(-\left[G^{\mathrm{A}} H^{-1} (G^{\mathrm{A}})^T\right]^{-1} \left[G^{\mathrm{A}} H^{-1} \alpha + W^{\mathrm{A}} + S^{\mathrm{A}} L\right]\right)_i, \quad \forall i \in \mathrm{A} \not/ \{1\} \tag{78}$$

$$W_i + S_i L \geq G_i \left[-H^{-1}\alpha + H^{-1}(G^{\mathrm{A}})^T \left[G^{\mathrm{A}} H^{-1} (G^{\mathrm{A}})^T \right]^{-1} \left[G^{\mathrm{A}} H^{-1}\alpha + W^{\mathrm{A}} + S^{\mathrm{A}} L \right] \right], \quad \forall i \in \mathrm{A} \not\parallel \{1\} \qquad (79)$$

Given the LICQ (75) and the diagonal form of the matrix H, $G^{\mathrm{A}} H^{-1} (G^{\mathrm{A}})^T$ is invertible. Equations (73) and (74) can then be used to derive explicit solutions for Λ^{A} and P as shown in equations (76) and (77). Note that these solutions are linear-affine functions of the load vector L.

In summary, given a particular load vector L, explicit solutions have been derived for P and Λ^{A} as linear-affine functions of L. However, by construction, as long as the set A of active constraints remains unchanged in a neighborhood of the load vector L in the load space L, the linear-affine form of these solutions remains optimal. Such a neighborhood is given by the feasible region determined from (71) and (72). Substituting Λ^{A} and P from equations (76) and (77) into (71) and (72), one obtains inequalities (78) and (79). The load vectors L satisfying the latter inequalities are the intersection of a finite number of half-spaces in the load space, and hence they form a convex polytope in this load space.

BIBLIOGRAPHY

[1] G. Li, C. C. Liu, C. Mattson, and J. Lawarrée, "Day-ahead electricity price forecasting in a grid environment," *IEEE Trans. Power Syst.*, vol. 22, no. 1, pp. 266-274, Feb. 2007.

[2] (2009, Feb.) Green power superhighways. [Online]. Available: http://seia.org/galleries/pdf/GreenPowerSuperhighways.pdf

[3] (2010, Mar.) A survey of transmission cost allocation issues, methods and practices. [Online]. Available: http://pjm.com/documents/media /documents/reports/20100310-transmission-allocation-cost-web.ashx

[4] A. Schumacher, A. Fink, and K. Porter, "Moving beyond paralysis: How states and regions are creating innovative transmission projects," National Renewable Energy Laboratory, MA, Tech. Rep. NREL/SR-550- 46691, Oct. 2009.

[5] (2009, Mar.) FERC revises policies to ease financing of merchant transmission projects. [Online]. Available: http://www.hunton.com/files/tbl_s10News/16070/ferc_revises_policies 3.3.09.pdf

[6] C. B. Berendt, "A state-based approach to building a liquid national market for renewable energy certificates: the REC-EX model," *The Electricity Journal*, vol. 19, issue 5, pp. 54-68, Jun 2006.

[7] H. Zareipour, C. A. Cañizares, K. Bhattacharya, and J. Thomson, "Application of public-domain market information to forecast Ontario's wholesale electricity prices," *IEEE Trans. Power Syst.*, vol. 21, no. 4, pp. 1707-1717, Nov. 2006.

[8] F. Nogales, J. Contreras, A. Conejo, and R. Espinola, "Forecasting next-day electricity prices by time series models," *IEEE Trans. Power Syst.*, vol. 17, no. 2, pp. 342–348, May 2002.

[9] J. Contreras, R. Espinola, F. J. Nogales, and A. J. Conejo, "ARIMA models to predict next-day electricity prices," *IEEE Trans. Power Syst.*, vol. 18, no. 3, pp. 1014–1020, Aug. 2003

[10] R. C. Garcia, J. Contreras, M. Akkeren, and J. B. C. Garcia, "A GARCH forecasting model to predict day-ahead electricity prices," *IEEE Trans. Power Syst.*, vol. 20, no. 2, pp. 867–874, May 2005.

[11] M. Shahidehpour, H. Yamin, and Z. Yi, *Market Operations In Electric Power Systems, Forecasting, Scheduling, and Risk Management*. New York: Wiley-Interscience, 2002.

[12] Y. Y. Hong and C. Y. Hsiao, "Locational marginal price forecasting in deregulated electricity markets using artificial intelligence," *IEE Proceedings-Generation Transmission and Distribution*, vol. 149, no. 5, pp. 621-626, Sept. 2002.

[13] N. Amjady, "Day-ahead price forecasting of electricity markets by a new fuzzy neural network," *IEEE Trans. Power Syst.*, vol. 21, no. 2, pp. 887-896, May 2006.

[14] Y.-Y. Hong and C.-F. Lee, "A neuro-fuzzy price forecasting approach in deregulated electricity markets", *Electric Power Systems Research*, vol. 7, pp. 3151–157, 2005.

[15] H. Y. Yamin, S. M. Shahidehpour, and Z. Li, "Adaptive short-term electricity price forecasting using artificial neural networks in the restructured power markets," *Electrical Power and Energy Systems*, vol. 26, pp.571–581, Oct. 2004.

[16] F. Gao, X. Guan, X.-R. Cao, and A. Papalexopoulos, "Forecasting power market clearing price and quantity using a neural network method," *Proc. IEEE Power Engineering Society Summer Meeting*, vol. 4, pp. 2183-2188, 2000.

[17] E. Ni and P. B. Luh, "Forecasting power market clearing price and its discrete PDF using a Bayesian-based classification method," *Proc. IEEE Power Engineering Society Winter Meeting*, vol. 3, pp. 1518-1523, 2001.

[18] J.D. Nicolaisen, C. W. Richter, and G. B. Sheble, "Price signal analysis for competitive electric generation companies," Proc. *Int. Conf. Electric Utility Deregulation and Restructuring and Power Technologies DRPT*, pp. 66-71, 2000.

[19] D. W. Bunn, "Forecasting loads and prices in competitive power markets," *Proc. of the IEEE*, vol. 88, no. 2, pp. 163-169, Feb. 2000.

[20] J. Bastian, J. Zhu, V. Banunarayanan, and R. Mukerji, "Forecasting energy prices in a competitive market," *IEEE Computer Applications in Power*, pp. 40-45, Jul. 1999.

[21] G. Li, C. C. Liu, and H. Salazar, "Forecasting transmission congestion using day-ahead shadow prices," *Proceedings IEEE PSCE 2006*, pp. 1705-1709, 2006.

[22] L. Min, S. T. Lee, P. Zhang, V. Rose and J. Cole, "Short-term probabilistic transmission congestion forecasting," *Proceedings IEEE DPRT 2008*, pp.764-770, Nanjing, China, April 2008.

[23] R. Bo and F. Li, "Probabilistic LMP forecasting considering load uncertainty," *IEEE Trans. Power Syst.*, vol 24, no. 3, pp. 911-922, Aug. 2009.

[24] F. Li and R. Bo, "Congestion and price prediction under load variation," *IEEE Trans. Power Syst.*, vol. 24, no. 2, pp. 1279-1289, May 2009.

[25] Q. Zhou, L. Tesfatsion, and C. C. Liu, "Global sensitivity analysis for the short-term prediction of system variables," *Proc. IEEE PES General Meeting 2010*, Mpls, MN, USA, July 26 - July 29, 2010.

[26] L. P. Garces, A. J. Conejo, R. Garcia-Bertrand, and R. Romero, "A bilevel approach to transmission expansion planning within a market environment," *IEEE Trans. Power Syst.*, vol. 24, no. 3, pp. 1513–1522, Aug. 2009.

[27] P. Maghouli, S. H. Hosseini, M. O. Buygi, and M. Shahidehpour, "A multi-objective framework for transmission expansion planning in deregulated environments," *IEEE Trans. Power Syst.*, vol. 24, no. 2, pp. 1051–1061, May 2009.

[28] S. de la Torre, A. J. Conejo, and J. Contreras, "Transmission expansion planning in electricity markets," *IEEE Trans. Power Syst.*, vol. 23, no. 1, pp. 238–248, 2008.

[29] I. J. Silva, M. J. Rider, R. Romero, and C. A. F. Murari, "Transmission network expansion planning considering uncertainty in demand," *IEEE Trans. Power Syst.*, vol. 21, no. 4, pp. 1565–1573, 2006.

[30] H. Yu, C. Y. Chung, K. P. Wong, and J. H. Zhang, "A chance constrained transmission network expansion planning method with consideration of load and wind farm uncertainties," *IEEE Trans. Power Syst.*, vol. 24, no. 3, pp. 1568–1576, 2009.

[31] R. Billinton and W. Wangdee, "Reliability-based transmission reinforcement planning associated with large-scale wind farms," *IEEE Trans. Power Syst.*, vol. 22, no. 1, pp. 34–41, 2007.

[32] E. Sauma and S. Oren, “Proactive planning and valuation of transmission investments in restructured electricity markets,” Journal of Regulatory Economics, vol. 30, pp. 358–387, 2006.

[33] J. Pan, Y. Teklu, S. Rahman, and K. Jun, “Review of usage-based transmission cost allocation methods under open access,” *IEEE Trans. Power Syst.*, vol. 15, no. 4, pp. 1218–1224, 2000.

[34] A. R. Abhyankar, S. A. Soman, and S. A. Khaparde, “Min-max fairness criteria for transmission fixed cost allocation,” *IEEE Trans. Power Syst.,* vol. 22, no. 4, pp. 2094–2104, 2007.

[35] H. A. Gil, F. D. Galiana, and A. J. Conejo, “Multiarea transmission network cost allocation,” *IEEE Trans. Power Syst.*, vol. 20, no. 3, pp. 1293–1301, 2005.

[36] H. A. Gil, F. D. Galiana, and E. L. da Silva, “Nodal price control: a mechanism for transmission network cost allocation,” *IEEE Trans. Power Syst.*, vol. 21, no. 1, pp. 3–10, 2006.

[37] P. R. Gribik, D. Shirmohammadi, J. S. Graves, and J. G. Kritikson, “Transmission rights and transmission expansions,” *IEEE Trans. Power Syst.,* vol. 20, no. 4, pp.728–1737, 2005.

[38] W. Shang and O. Volij, “Transmission investment cost allocation within the cooperative game framework,” in *Proc. IEEE PES Power Systems Conf. and Exposition PSCE ’06,* 2006, pp. 1971–1977.

[39] F. J. Rubio-Oderiz and I. J. Perez-Arriaga, “Marginal pricing of transmission services: a comparative analysis of network cost allocation methods,” *IEEE Trans. Power Syst.*, vol. 15, no. 1, pp. 448–454, 2000.

[40] J. H. Roh, M. Shahidehpour, and Y. Fu, "Market-based coordination of transmission and generation capacity planning," *IEEE Trans. Power Syst.*, vol. 22, no. 4, pp. 1406–1419, 2007.

[41] P. Joskow and J. Tirole, "Merchant transmission investment," *The Journal of Industrial Economics*, pp. 233–264, 2005.

[42] H. Salazar, C. C. Liu, and R. F. Chu, "Decision analysis of merchant transmission investment by perpetual options theory," *IEEE Trans. Power Syst.*, vol. 22, no. 3, pp. 1194–1201, 2007.

[43] H. Salazar, C. C. Liu, and R. F. Chu, "Market-based rate design for recovering merchant transmission investment," *IEEE Trans. Power Syst.*, vol. 25, no. 1, pp. 305–312, 2010.

[44] Q. Zhou, L. Tesfatsion, and C. C. Liu, "Short-term congestion forecasting in wholesale power markets", *IEEE Trans. Power Syst.*, to appear.

[45] A. Bemporad, M. Morari, V. Dua, and E. N. Pistikopoulos, "The explicit linear quadratic regulator for constrained systems," *Automatica*, vol. 38, pp. 3-20, 2002.

[46] P. Tøndel, T. A. Johansen, and A. Bemporad, "An algorithm for multi-parametric quadratic programming and explicit MPC solutions," *Automatica*, vol. 39, pp. 489-497, 2003.

[47] M. Berg, M. Kreveld, M. Overmars, and O. Schwarzkopf, *Computational Geometry: Algorithms and Applications*. Berlin, New York: Springer, 2000.

[48] MISO Fact Sheet. [Online]. Available: http://www.midwestiso.org/

[49] F. P. Preparata and M. I. Shamos, *Computational Geometry: An Introduction*. New York: Springer-Verlag, 1985.

[50] C. B. Barber, D. P. Dobkin, and H. T. Huhdanpaa, "The Quickhull Algorithm for Convex Hulls," *ACM Transactions on Mathematical Software*, vol. 22, no. 4, pp. 469-483, Dec. 1996.

[51] Qhull. [Online]. Available: http://www.qhull.org/.

[52] S. S. Skiena, *The Algorithm Design Manual. London*, Springer, 2008.

[53] *AMES Wholesale Power Market Test Bed: Homepage*. [Online]. Available at http://www.econ.iastate.edu/tesfatsi/AMESMarketHome.htm

[54] H. Li and L. Tesfatsion, "The AMES wholesale power market test bed:A computational laboratory for research, teaching, and training," *Proc., IEEE Power and Energy Society General Meeting*, Calgary, Alberta, CA, July 26-30, 2009.

[55] MISO Website. [Online]. Available: http://www.midwestiso.org

[56] NYISO map. [Online]. Available:http://www.ferc.gov/images/marketoversight/mkt-electric/regmaps/2007_ny_elect_map.gif

[57] NYISO Market Data. [Online]. Available: http://www.nyiso.com/public /marketsoperations/market/data/pricingdata/index.jsp

[58] F. Rahimi. Market metrics for DOE congestion study: overview and results.[Online].Available:http://www.congestion09.anl.gov/documents/docs/techws/ Rahimi.pdf

[59] I. Yaniv and D. P. Foster, "Graininess of judgment under uncertainty: an accuracy-informativeness trade-off," *Journal of Experimental Psychology*, General 124, pp.424-432, 1995.

[60] R. Wiser and M. Bolinger, "Renewable energy RFPs: Solicitation response and wind contract prices," Lawrence Berkeley National Laboratory, 2005.

[61] J. F. Nash, “The bargaining problem,” *Econometrica,* vol. 18, no. 2, pp. 155–162, 1950. [Online]. Available: http://www.jstor.org/ stable/1907266

[62] J. Nash, “Two-person cooperative games,” *Econometrica*, vol. 21, no. 1, pp. 128–140, 1953.

[63] K. Binmore, A. Rubinstein, and A. Wolinsky, “The Nash bargaining solution in economic modeling,” *The RAND Journal of Economics*, vol. 17, no. 2, pp. pp. 176–188, 1986. [Online]. Available: http://www.jstor.org/stable/2555382

[64] L. Tesfatsion, “Games, goals, and bounded rationality,” *Theory and Decision*, vol. 17, pp. 149–175, 1984.

[65] P. C. Roth and D. A. R. Gpa, “Bargaining experiments,” *Handbook of Experimental Economics.* Princeton University Press, 1995, pp. 253–348

[66] Q. Zhou, L. Tesfatsion, and C. C. Liu, "Scenario generation for price forecasting in restructured wholesale power markets", *Proc. IEEE PES Power Systems Conf. and Exposition PSCE ’09*, Seattle, WA, March 15-18, 2009.

LIST OF PUBLICATIONS

Q. Zhou, L. Tesfatsion, and C. C. Liu, "Short-term congestion forecasting in wholesale power markets," *IEEE Transactions on Power Systems*, to appear.

Q. Zhou, L. Tesfatsion, C. C. Liu, and R. Chu, "A Nash Bargaining approach for transmission investment to integrate renewable energy," *IEEE Transactions on Power Systems*, to be submitted.

Q. Zhou, L. Tesfatsion, and C. C. Liu, "Global sensitivity analysis for the short-term prediction of system variables," *IEEE Power & Energy Society General Meeting 2010*, Minneapolis, Minnesota, July 2010.

Q. Zhou, L. Tesfatsion, and C. C. Liu, "Scenario generation for price forecasting in restructured wholesale power markets," *IEEE Power Systems Conference & Exposition 2009*, Seattle, WA, March 2009.

Q. Zhou, C. Mao, J. Lu, H. Liu, and H. Wang, "Digital simulation of power system load," *Proceedings of the CSU-EPSA*, vol. 20, no.3, Jun. 2008.